

Influence of the Solarus AB reflector geometry and position of receiver on the output of the concentrating photovoltaic thermal collectors

Victor Seram

Thesis to obtain the Master of Science Degree in
Energy Engineering and Management

Supervisors: Prof. Carlos Alberto Ferreira Fernandes
Prof. João Paulo Neto Torres

Examination Committee

Chairperson: Prof. Luís Filipe Moreira Mendes

Supervisor: Prof. João Paulo Neto Torres

Member of the Committee: Prof. Paulo José da Costa Branco

December 2017

ACKNOWLEDGEMENTS

The thesis work would not have been possible without the help and support of all the people who has contributed their time and effort.

First and foremost, I am greatly thankful and indebted to my supervisors, Prof. Carlos Alberto Ferreira Fernandes and Asst. Prof. João Paulo Neto Torres for their advices and never ending patience and caring providing me the best support. Their regular inputs and guidance was a constant drive and motivation to work towards my goal. I could not be more grateful for the freedom given to me to work on my own pace to learn and explore the unknown regions through my own lenses.

I would also like to thank Solarus for letting me work on their project and research topic which I believe will be a big cause for the future.

Finally, I would like to thank InnoEnergy, KIT and IST for giving me this platform to learn and grow as an engineer.

Abstract:

Solar energy, if harnessed efficiently can provide the world with clean and reliable power supply. Solarus AB₁ manufactures hybrid solar PVT which provides both thermal and electrical energy using a unique design of asymmetric parabolic collector called MaReCo or Maximum Reflector Collector. The main goal of the thesis is to study, model and characterise suitable designs for a concentrating PVT collector at different locations on the globe to optimise the power at the receiver without cost penalties of the overall system. The power output on the receiver of the solar collector is analysed with respect to the time of the year, the inclination angle of the collector and also the hourly variation of the day. With standard MaReCo simulations are performed at Gävle, Lisbon and Delhi observing the change in the output as the latitude decreases gradually. It has been found that with a little orientation change in the system for lower latitude places, the performance of MaReCo improved further. A modified MaReCo model is also introduced and simulated at Lisbon and Gävle checking its feasibility and usability. Due to easier availability of solar energy and larger market potential, simulations are made at Nairobi and Lisbon and compared. Two types of symmetrical parabolic collectors are designed for such simulations. The parabolic collector with side edge receiver is found to be the best suitable collector at the equatorial region for all the season.

Keywords: MaReCo; parabolic collectors; inverted orientation;

RESUMO

A energia solar, quando aproveitada de forma eficiente, contribui para a geração de energia de uma forma segura e limpa do ponto de vista ambiental. A *Solarus AB* manufatura painéis *PVT* híbridos que fornecem simultaneamente energia elétrica e térmica, utilizando coletor de design único com um formato parabólico assimétrico designado por *MaReCo* ou *Maximum Reflector Collector*. O principal objetivo desta tese é estudar e projetar diferentes formatos para um concentrador *PVT* para diferentes pontos do globo tendo, como intuito, otimizar a potência no painel solar sem que para isso existam custos acrescidos ao sistema. A potência gerada e o número de fótons incidentes no painel são analisados detalhadamente tendo em conta o período do ano em questão, a inclinação do coletor, bem como a variação horária. Com a geometria do *MaReCo*, foram feitas simulações para as regiões de Lisboa, Gävle e Delhi. Provou-se que com uma pequena variação na orientação no sistema, para regiões de menor latitude, o desempenho da geometria *MaReCo* aumenta. Foi também introduzido e simulado um modelo modificado do *MaReCo* em Lisboa e Gävle, testando viabilidade e usabilidade. Devido a uma mais fácil disponibilidade de energia solar e um maior potencial de mercado, foram feitas e comparadas simulações nas regiões de Nairobi e Lisboa. Foram desenvolvidos dois tipos de coletores parabólicos simétricos para tais simulações. Comprovou-se que a solução com coletor parabólico e os painéis na ponta da estrutura, é a melhor para as regiões equatoriais durante todo o ano.

Palavras Chave: *MaReCo*; coletor parabólico; orientação invertida;

Contents

Figures.....	VII
Tables.....	X
Symbols.....	XI
Abbreviations.....	XII
1. Introduction.....	1
1.1. Outline.....	2
1.2. Thesis goals.....	2
1.3. Solar Radiation.....	2
1.3.1. The sun.....	2
1.3.2. Solar constant.....	3
1.3.3. Extraterrestrial radiation.....	3
1.3.3.1. Spectral distribution of extraterrestrial radiation.....	4
1.3.3.2. Variation of extraterrestrial radiation.....	4
1.4. Solarus AB.....	5
1.4.1. The company.....	5
1.4.2. Products.....	6
2. Background	7
2.1. The solar collector.....	7
2.1.1. Flat-plate collectors.....	7
2.1.2. Concentrating collectors.....	8
2.1.2.1. Types of concentrating solar collector.....	8
2.1.2.2. Compound Parabolic Collector (CPC).....	11
2.1.2.3. Maximum Reflector Collector (MaReCo).....	12
2.1.2.3.1. Structure of MaReCo.....	12
2.1.2.3.2. MaReCo Prototypes	13
2.2. Solarus PowerCollectors.....	15
2.2.1. C-PVT.....	16
2.2.2. C-T.....	17
3. Numerical study method.....	18
3.1. Collector Simulations.....	18
3.1.1. Tonatiuh Program.....	18
3.1.2. Mathematica Program.....	20
3.2. Design of the MaReCo structure with Tonatiuh.....	20
3.2.1. Design of roof integrated MaReCo.....	20
3.2.1.1. Structure of the collector.....	20
3.2.1.2. Orientation of the collector.....	21
3.2.1.3. Time structure.....	23
3.2.1.4. Solar rays.....	23
3.2.2. Design of modified MaReCo model.....	23

3.2.3.	Design of Parabolic collector with receiver at the side edge.....	23
3.2.4.	Design of Parabolic collector with receiver at the focus.....	24
3.3.	Post processing with Mathematica.....	25
4.	Results and discussions.....	28
4.1.	Roof-integrated MaReCo.....	28
4.1.1.	Lisbon.....	28
4.1.1.1.	Comparison of power with respect to tilt angle.....	28
4.1.1.2.	Orientation change of MaReCo.....	30
4.1.1.2.1.	Inverted orientation in summer.....	31
4.1.1.2.2.	Inverted orientation in spring, fall and winter.....	32
4.1.1.3.	Flux distribution at the receiver	33
4.1.2.	Gävle.....	33
4.1.2.1.	Comparison of Power with respect to tilt angle.....	33
4.1.2.2.	Gävle summer with tilt 30° vs tilt 35°.....	34
4.1.2.3.	Gävle with inverted orientation.....	35
4.1.3.	Delhi.....	36
4.1.3.1.	Comparison of Power with respect to tilt angle.....	36
4.1.3.2.	Delhi with inverted orientation in summer.....	37
4.1.3.3.	Comparison of daily power curve with Lisbon in summer.....	38
4.1.3.4.	Delhi with inverted orientation in spring, fall and winter.....	39
4.2.	Modified roof integrated MaReCo.....	39
4.2.1.	Comparison of power with respect to the tilt angle.....	39
4.2.2.	Hourly simulation in summer.....	40
4.2.3.	Flux distribution on the receiver.....	40
4.2.4.	Inverted orientation of modified roof integrated MaReCo.....	41
4.2.4.1.	Power vs inclination angle for spring, summer and fall.....	41
4.3.	Parabolic collector with receiver at the side edge.....	41
4.3.1.	Lisbon.....	42
4.3.1.1.	Simulations with normal and inverted orientation in summer.....	42
4.3.1.2.	Comparison of power with respect to inclination angle.....	42
4.3.1.3.	Flux distribution on the receiver.....	43
4.3.2.	Nairobi.....	44
4.3.2.1.	Comparison of power with respect to inclination angle.....	44
4.3.2.2.	Flux distribution on the receiver.....	44
4.4.	Parabolic collector with receiver at the focus	45
4.4.1.	Lisbon.....	45
4.4.1.1.	Comparison of power with respect to inclination angle.....	45
4.4.1.2.	Flux distribution on the receiver.....	46
4.4.2.	Nairobi.....	46
4.4.2.1.	Comparison of power with respect to inclination angle.....	46

4.4.2.2. Comparison of parabolic collector with horizontal middle receiver with modified MaReCo.....	47
4.4.2.3. Flux distribution on the horizontal middle receiver of the parabolic collector.....	48
4.5. Comparison	48
4.6. Proposal.....	50
5. Future work.....	52
6. Conclusion.....	53
7. Bibliography.....	55

Figures

Figure 1.1: The Sun.....	3
Figure 1.2: Sun-earth relationship.....	3
Figure 1.3: WRC standard spectral irradiance curve.....	4
Figure 1.4 Variation of extraterrestrial radiation with time of year.....	4
Figure 1.5 Solarus logo.....	5
Figure 1.6 Comparison of PowerCollector with conventional PV	5
Figure 1.7 What the company offers at present	6
Figure 2.1 Flat-plate collector	7
Figure 2.2 Concentrating Collector sketch	8
Figure 2.3 Diagram of Parabolic trough	9
Figure 2.4 Diagram of Solar tower	9
Figure 2.5 Components of Parabolic dish	10
Figure 2.6 Diagram of linear Fresnel collector	10
Figure 2.7 Compound Parabolic Collector	11
Figure 2.8 Basic structure of MaReCo	13
Figure 2.9 Diagram of stand-alone MaReCo (for Stockholm conditions with cover glass angle of 30°).....	13
Figure 2.10 Diagram of roof integrated MaReCo	14
Figure 2.11 Diagram of east/west MaReCo with 70° optical axis from the cover glass	14
Figure 2.12 Diagram of spring/fall MaReCo for roof tilt 30°	15
Figure 2.13 Diagram of wall MaReCo designed for south facing with optical axis at 25° from the horizon	15
Figure 2.14 Solarus PowerCollector showing the upper and lower receiver	16
Figure 2.15a Single PowerCollector C-PVT side view	16
Figure 2.15b PowerCollector C-PVT silver	16
Figure 2.16 PowerCollector C-T	17
Figure 3.1 Tonatiuh logo	18
Figure 3.2 Wolfram Mathematica logo	20
Figure 3.3 Roof integrated MaReCo showing the circular reflector and the lower parabolic reflector.....	20
Figure 3.4 Roof integrated MaReCo with dimensions.....	21
Figure 3.5 Diagram of a solar panel in Los Angeles (latitude: 34° N) facing south.....	22
Figure 3.6 Modified model of the roof integrated MaReCo.....	24
Figure 3.7 Parabolic collector with receiver at side edge	24
Figure 3.8 Parabolic collector with horizontal receiver at the focus.....	25
Figure 3.9 Information inside an ASCII file.....	25
Figure 3.10 Mathematica code	26
Figure 4.1 Comparison of the power during 21 st June, 20 th March, 22 nd Sept and 21 st Dec at the receiver in Lisbon at 12.00 with inclination angle of the collector ranging from 0° to 65°.....	28
Figure 4.2 Hourly power production in Lisbon at June 21 st with collector inclination angle 10°.....	29

Figure 4.3a Normal orientation of MaReCo at Lisbon.....	30
Figure 4.3b Inverted orientation of MaReCo at Lisbon.....	30
Figure 4.4. Power output (12.00 hour) vs inclination of the inverted MaReCo in Lisbon at June 21 st	31
Figure 4.5 Hourly power output with fixed inclination angle at 15° (maximum power output angle) in Lisbon during 21 st June	31
Figure 4.6 Power output (at 12.00) vs inclination angle in Lisbon during 22 nd Sept and 20 th March ...	32
Figure 4.7 Flux distribution during summer at Lisbon.....	33
Figure 4.8 Comparison of power during 21 st June, 20 th March and 22 nd Sept at the receiver in Gävle at 12.00 with inclination angle of the collector ranging from 0° to 65°.....	34
Figure 4.9 Power output (12.00 hour) vs time of day at Gävle in summer with tilt angle 30° vs tilt angle 35°	35
Figure 4.10 Comparison of the power during 21 st June, 20 th March, 22 nd Sept and 21 st Dec at the receiver in Delhi at 12.00 with collector tilt angle ranging from 0° to 65°.....	36
Figure 4.11 Delhi on 21 st June.....	37
Figure 4.12. Power output (at 12.00 hour) vs inclination curve in Delhi with inverted orientation of the solar MaReCo.....	37
Figure 4.13 Hourly power output variation in summer in Delhi vs Lisbon.....	38
Figure 4.14 Position of the sun from rising till setting in Delhi and Lisbon.....	38
Figure 4.15 Comparison of the power during 21 st June, 20 th March, 22 nd Sept and 21 st Dec at the receiver in Lisbon at 12.00 with inclination of angle of the collector ranging from 0° to 85°.....	39
Figure 4.16 Hourly power output (kW) in 21 st June in Lisbon at 15° collector inclination.....	40
Figure 4.17 Flux distribution on 21 st June in Lisbon.....	40
Figure 4.18 Comparison of the power during 21 st June, 20 th March and 22 nd Sept at the receiver in Lisbon at 12.00 with inclination of angle of the collector ranging from 0° to 50°	41
Figure 4.19a. Power vs inclination with normal orientation	42
Figure 4.19b. Lisbon, inverted orientation.....	42
Figure 4.20 Comparison of the power during 20 th March, 22 nd Sept and 21 st Dec at the receiver in Lisbon at 12.00 with inclination angle of the collector ranging from 0° to 65°	43
Figure 4.21 Flux distribution during summer on side edge receiver of parabolic collector in Lisbon ...	43
Figure 4.22 Comparison of the power during 21 st June, 20 th March, 22 nd Sept and 21 st Dec at the receiver in Nairobi at 12.00 with inclination angle of the collector ranging from 0° to 65°	44
Figure 4.23 Flux distribution during summer on side edge receiver of parabolic collector in Nairobi ..	45
Figure 4.24. Comparison of the power during 21 st June, 20 th March, 22 nd Sept and 21 st Dec at the receiver in Lisbon at 12.00 with inclination angle of the collector ranging from 0° to 90°	45
Figure 4.25 Flux distribution on 21 st June in Lisbon	46
Figure 4.26 Comparison of the power during 21 st June, 20 th March, 22 nd Sept and 21 st Dec at the receiver in Nairobi at 12.00 with inclination angle of the collector ranging from 0° to 50°.....	47
Figure 4.27 Comparison of the power during 21 st June, 20 th March, 22 nd Sept and 21 st Dec at the receiver in Nairobi at 12.00 with inclination angle of the collector ranging from 0° to 40°.....	47

Figure 4.28 Flux distribution on 21st in Nairobi.....48

Tables

Table 1. The maximum power output tilt angle for spring, summer, fall and winter.....	29
Table 2. Hourly power output at the receiver with 40° tilt angle of the solar collector in winter in Lisbon	30
Table 3 shows the hourly power received by the roof integrated MaReCo at Lisbon during 21 st June from 9:00 to 18:00 hour. The power received is recorded as kW.....	32
Table 4 shows the power output (kW) at 12.00 at the receiver with tilt angle ranging from 0° to 60° during summer at Gävle with the inverted orientation.....	36
Table 5. The same graph is depicted showing the amount of photons received on the receiver.	41
Table 6. Comparison between the designs.....	48
Table 7. Comparison between normal and inverted orientation of roof integrated MaReCo.....	49

Symbols

G_{sc}	Solar constant (Watt/m ²)
G_{on}	Extraterrestrial radiation (Watt/m ²)
Q_u	Useful output (Joule)
A_c	Collector area (m ²)
S	radiation absorbed by the collector per unit area of collector (incorporating the optical losses) (Joule/m ²)
U_L	Overall loss coefficient
T_{pm}	Mean plate temperature (K)
T_a	Ambient temperature (K)
C_i	Concentration factor
A_{abs}	Absorber area (m ²)
A_c	Aperture area (m ²)
W_{th}	Thermal power (watt)
W_{el}	Electrical power (watt)
θ	Angle rotated to align the collector in east-west direction (degree and radian)
γ	Tilt angle (degree and radian)
q,r,t	Vectors
x, y, z, w	Quaternion variables
i	Number of files
φ	Aperture tilt angle (degree and radian)
β	Absorber inclination angle (degree and radian)

Abbreviations

PV: Photo Voltaic

CSP: Concentrated Solar Power

RES: Renewable Energy Sources

PVT: Photovoltaic Thermal

WRC: World Radiation Centre

MaReCo: Maximum Reflector Collector

C-PVT: Concentrated Photovoltaic and thermal collector

C-T: Concentrated Thermal collector

ACC: Active Cell Cooling

DOE: Department of Energy

NREL: National Renewable Energy Laboratory

MURA: Minority Research Associate

GUI: Graphic User Interface

UT: Universal Time

CT: Central Time

1. Introduction:

Modernisation plays a huge role in the change of behaviour of the people. The behaviour towards energy, not only in production but also in the consumption. Conventional ways of generating power includes mostly of fossil fuel based starting from coal based steam plant to nuclear power plants. Global warming is real. As men are more exposed to the actual truth of the planet and the threat it possesses in a long run, serious steps are taken like the Paris climate agreement. However taking a glance at the present situation regarding the production of power and energy, renewable resources plays a massive part in main stream energy production and feed in the grid. By the end of 2016, 303 GW of PV have been installed all over the world, 16 countries installed at least 500 MW of PV, Germany ranks first in solar PV per capita with 511 watt/capita [1]. Renewable energy sources (RES) share of gross German electricity production in 2015 was 30.7% [2].

The world energy consumption at the moment is 10 terawatts (TW) per year. By the year 2050 the expected energy consumption would be 30 TW. The conclusion is an additional 20 TW of CO₂ free energy source is required to balance the demand. One solution to stabilize CO₂ might be to use photovoltaics (PV) and other renewables like hydro and wind for electricity (10 TW), hydrogen for the transportation (10 TW), and fossil fuels for residential and industrial heating (10 TW) [3]. Hence solar energy (photovoltaics) will play an important role in meeting the world future energy demand. The present is considered as the “tipping point” for PV [4].

Solar energy, an inexhaustible resources, clean and non-polluting as it may have seen, is not an easy task to make the most out of it. Its potential lies in the method and the techniques used for the maximum efficiency possible. Various means have been developed to harness the solar energy. Flat-plate solar panels and concentrated solar power (CSP) systems are some of the ways to generate power from the sun. CSP technologies use mirrors to focus or concentrate the light energy from the sun into a small area to generate heat which then creates steam to drive a turbine that generates electric power [5].

Photovoltaic thermal (PVT) hybrid system is the combination of the above mentioned methods. A combined hybrid PV and solar-thermal system is an alternative environmentally friendly way which offers both thermal (e.g. water heating), as well as electrical output from a single unit. If designed correctly it gives a better efficiency compared to stand-alone PV modules. The system allows the simultaneous acquisition of both electrical and thermal outputs while at the same time reducing the losses in the electrical efficiency of the PV module because of the increase in temperature from the solar radiation. The reduction of loss is achieved due to the use of coolant (water flow) through the solar collector unit [6].

MaReCo or Maximum Reflector Collector is an asymmetrical solar collector used in PVT hybrid systems. Different types of MaReCo have been developed according to the conveniences e.g. stand-alone, roof or wall mounting. One of the main advantage of MaReCo is the cost reduction by replacing the expensive absorber area with inexpensive reflector area and concentrate the incoming solar radiation. The delivered energy output of the MaReCo is generally lower per aperture area than the flat plate collector. However, it is designed to fit the asymmetrical solar radiation distributions places like

Sweden. The main purpose of the thesis is to analyse the extent and limitations of MaReCo with respect to the location of the place on the globe and ways to improve the performance without any extra cost and major complications. Remodelling of the standard MaReCo is done and compared with the previous design. The potential of solar power lies in the equatorial region where the position of the sun rarely changes. Symmetrical parabolic collectors with varying receiver positions are simulated in such regions and analysed for the best situation and condition. Detailed studies of the annual solar radiation distribution has been done at different angles of incidence in order to maximise the power output and collect a higher percentage of the available solar radiation.

1.1. Outline:

The document follows the given pattern below:

Section 1 talks about the introduction of the master thesis and the general idea behind the present situation in the world regarding renewable energy and the fundamentals of solar energy;

Section 2 describes about the background of solar collectors and a detailed discussion about the different prototypes of MaReCo;

Section 3 describes about the simulation methods and the software used in doing so;

Section 4 describes the results and comparison between different geographical places alongside optimising the design and the discussions behind the obtained results;

Section 5 presents the recommendations and probable future work to improve the design;

Section 6 summarises and gives a conclusion on the thesis work;

1.2. Thesis goal:

- Study, modelling and characterization of suitable designs for a concentrating PVT collector taking into account the influence of its several constituents in order to optimize the power in the receiver without cost penalties of the overall system;
- Analyse the in-depth details behind the effectiveness of the position of the receiver with respect to the use of the collector in different location on earth;
- Analyse the suitability and feasibility of the collector designs in different locations on the planet;
- Evaluate the annual effectiveness of the collector;

1.3. Solar Radiation:

1.3.1. The sun:

The sun is a huge yellow sphere of intensely hot gaseous matter. Its diameter is 1.39×10^9 m and at an average distance of 1.5×10^{11} m from the earth. It has a blackbody temperature of 5777 K. The sun is the state of continuous fusion reactor with its constituent gases. Several fusion reactions supply the energy radiated by the sun from which the most important one is the process in which the four protons of hydrogen combines to form one helium nucleus. Since the mass of helium is lesser than that of the four hydrogen protons, the lost mass converts into massive energy. [7]

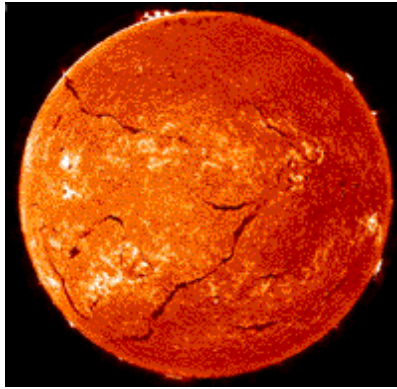


Figure 1.1: The Sun [8]

1.3.2. Solar Constant:

“The solar constant, G_{sc} , is the energy from the sun per unit time received on a unit area of surface perpendicular to the direction of propagation of the radiation at mean earth-sun distance outside the atmosphere” [7]. Figure 1.2 shows the schematic geometry of the sun-earth relationships. Due to the mean earth-sun distance of 1.5×10^{11} m, the sun obtains an angle of 32° with respect to the earth

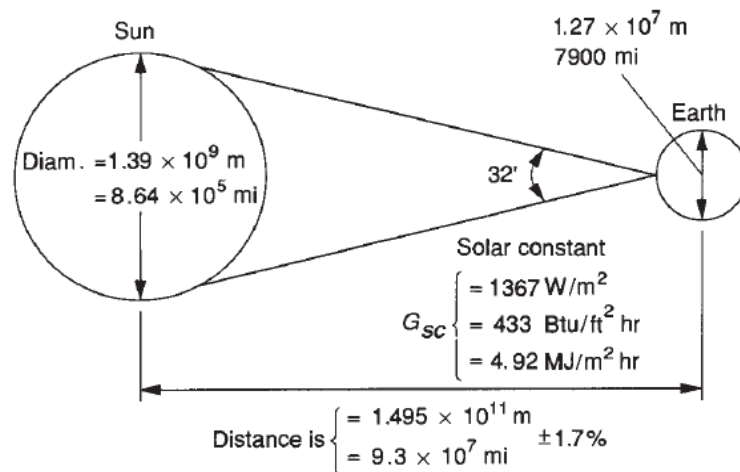


Figure 1.2: Sun-earth relationship [7]

Estimation of the solar constant were made from ground-based measurements far before rockets and spacecraft existed. Measurements were made from high mountains which were based on estimates of atmospheric transmission in various portions of the solar spectrum.

However, after the advent of modern technologies, balloons, high altitude aircrafts and rockets, the solar constant has been updating continuously from studies to studies. The World Radiation Centre (WRC) has adopted a solar constant, G_{sc} , value of 1367 W/m^2 with a correction factor of 1% [7].

1.3.3. Extraterrestrial radiation:

The solar radiation incident outside the earth’s atmosphere is known as extraterrestrial radiation. The average value of extraterrestrial irradiance is 1367 W/m^2 [9].

1.3.3.1. Spectral distribution of extraterrestrial radiation:

A compilation of standard spectral irradiance curve has been done based on high-altitude and space measurements. The World Radiation Centre (WRC) standard is shown in the Figure 1.3 below:

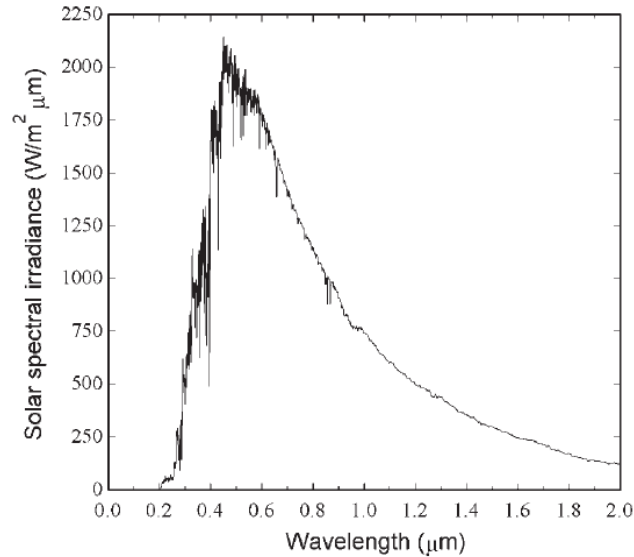


Figure 1.3: WRC standard spectral irradiance curve [7]

1.3.3.2. Variation of extraterrestrial radiation:

The variations in the radiation can be described in the following points.

Firstly is the variation in to the radiation emitted by the sun. Small variations of $\pm 1.5\%$ with different periodicities and variations related to sunspots are being suggested.

Secondly, variation in the earth-sun distance leads to the variations in the extraterrestrial radiation. It varies in the range of $\pm 3.3\%$.

Thirdly, the variation in the extraterrestrial radiation depends on the time of the year which is shown below in Figure 1.4

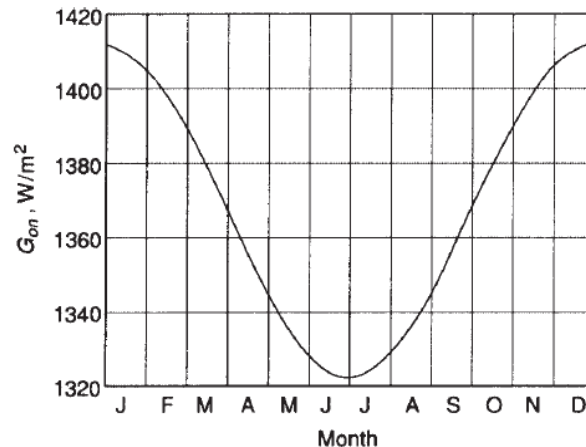


Figure 1.4 Variation of extraterrestrial radiation with time of year [7]

A near accurate value of extraterrestrial radiation incident on the plane normal to the radiation on the n^{th} day of the year is given by the first equation from (1) whereas second equation from (1) gives a more accurate result ($\pm 0.01\%$)

$$G_{on} = \begin{cases} G_{sc} \left(1 + 0.033 \cos \frac{360n}{365} \right) \\ G_{sc} (1.000110 + 0.034221 \cos B + 0.001280 \sin B + 0.000719 \cos 2B + 0.000077 \sin 2B) \end{cases} \quad (1)$$

Where, G_{on} is the extraterrestrial radiation incident on the plane normal to the radiation on the n^{th} day of the year and B is given by

$$B = (n - 1) \frac{360}{365} \quad (2)$$

1.4. Solarus AB

1.4.1. The company

Solarus is a new kind of innovative renewable energy company. The company is originally from Sweden but the headquarters is located in Venlo, the Netherlands since January 2015. The company logo is shown in the Figure 1.5



Figure 1.5 Solarus logo [10]

Solarus develop and market PowerCollector, a hybrid concentrated photovoltaic and thermal (C-PVT) collector and a C-T Thermal collector. The company supplies clean and affordable heat and electrical energy for residential and industrial customers. The PowerCollectors from Solarus are able to capture four times more solar energy than the conventional solar photovoltaic products on the market.



Figure 1.6 Comparison of PowerCollector with conventional PV [11]

The PowerCollector offers six solution for various applications in which today the focus is on heating, cooling and supplying electricity. In near future the company intends to focus in desalination, purification and steam applications.

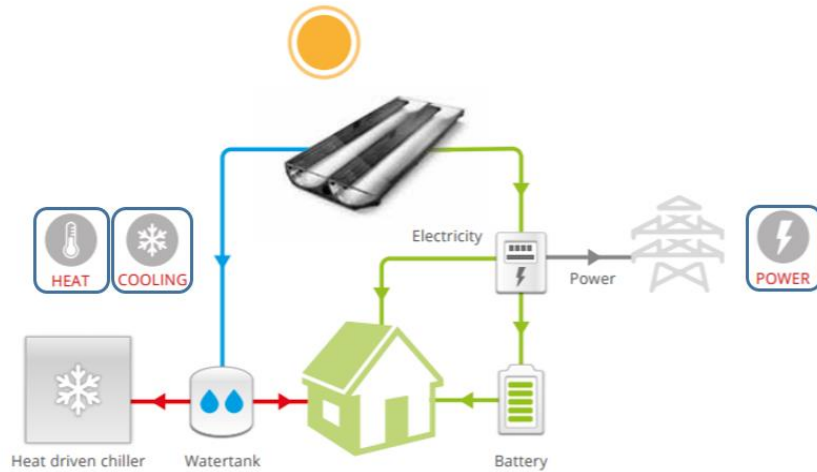


Figure 1.7 What the company offers at present [11]

Some of the important projects where PowerCollectors are being used as a source of energy are:

- In a hospital in Sweden, the operation room is powered, heated and cooled by the PowerCollector
- In Auroville Temple in India, the sun cooks more than 1000 meals a day [11]

1.4.2. Products

Solarus develops and markets three types of solar energy systems:

- Thermal
- PV (Photovoltaic)
- PVT (Photovoltaic-Thermal) hybrid solar collectors

MaReCo or Maximum Reflection Concentrator collectors are seasonal adapted. Hence the collector can be used almost all year round fulfilling the annual energy needs with the solar energy. The Solarus collector or the PowerCollector has a very low weight and low material content. It can concentrate sunlight 3.5 times and follow the movement of the sun throughout the year without the need for heliostat structure. Due to its unique seasonal adjustment features, it gives the highest efficiency even when the sun is low in the sky. This makes MaReCo feasible for all year round applications [12].

2. Background

2.1. The solar collector

“The sun provides more energy in four hours than the human race consumes in all forms in an entire year” [11]. To harness this solar energy, solar collectors are used. The solar collectors convert the solar energy to either electricity (Photovoltaic) or heat (Thermal) or both (PV-T). Solar collectors are mainly of two types: flat-plate collectors and concentrating collectors. Most of the simulations performed in this thesis are focused mainly on concentrated collectors.

2.1.1. Flat-plate collectors

A typical flat-plate collector is shown in Figure 2.1. A flat-plate collector is a metal box with a glass or plastic cover known as glazing on the top and a dark-coloured absorber plate on the bottom. The sides and the bottom are normally insulated to minimize heat loss. To protect the absorber from rain and dust is another reason why the absorber is put inside a box [13].

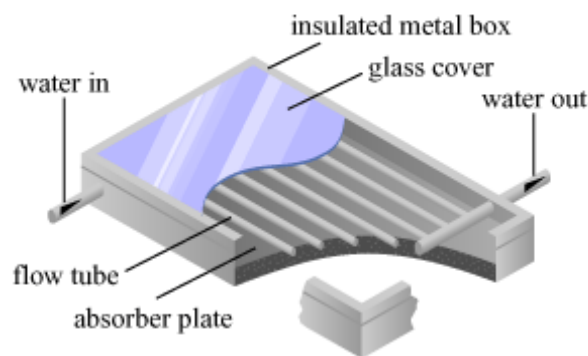


Figure 2.1 Flat-plate collector [14]

The sunlight which passed through the glazing cover strikes and heats up the absorber plate converting the solar energy to heat energy. The heat energy is then transferred to the liquid used in the absorber pipes attached to the absorber plates. ‘Selective coatings’ are usually painted on the absorber plates. This coating helps in better absorption and retaining of heat, even better than the ordinary black paint [13].

Optical and thermal losses are the criteria on which the efficiency of a solar flat plate collector depends according to the basic energy balance equation (3) [7].

$$Q_u = A_c[S - U_L(T_{pm} - T_a)] \quad (3)$$

Where,

Q_u is the useful output

A_c is the collector area

S is the radiation absorbed by the collector per unit area of collector (incorporating the optical losses)

U_L is the overall loss coefficient

T_{pm} is the mean plate temperature

T_a is the ambient temperature

2.1.2. Concentrating collectors

A very basic concentrating collector is shown in the Figure 2.2 below.

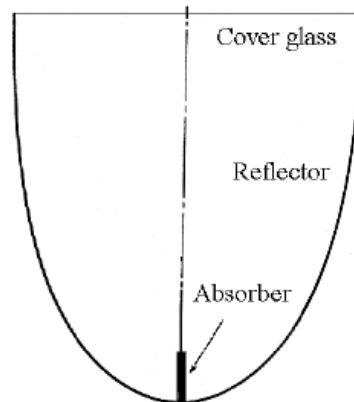


Figure 2.2 Concentrating Collector sketch [15]

The concentrating reflector reflects the incoming light from the sun and directs towards the absorber where it is then transferred to the heat carrying medium. The area of the absorber is reduced due to the reason that the concentration of the solar energy makes the absorber very hot. The concentration factor of the light depends on the following equation

$$C_i = \frac{A_{abs}}{A_c} \quad (4)$$

Where,

A_{abs} is the absorber area

A_c is the aperture area [15]

2.1.2.1. Types of concentrating solar collector:

Solar concentrating collectors cannot focus diffused sky radiation onto the absorber and most of the collectors require mechanical equipment that constantly orients the collector towards the sun and keep the absorber align to the focus. Hence it is classified as the following.

(i) Parabolic trough

Thermally efficient receiver tubes are placed in the focal line of the parabolic trough-shaped mirror which reflects the sunlight directly to the receiver pipes. Heat transfer takes place and fluid is circulated through a series of heat exchangers. An approximate temperature of 400°C is reached inside the receiver tube [16]. A detailed diagram of the collector is shown in the Figure 2.3.

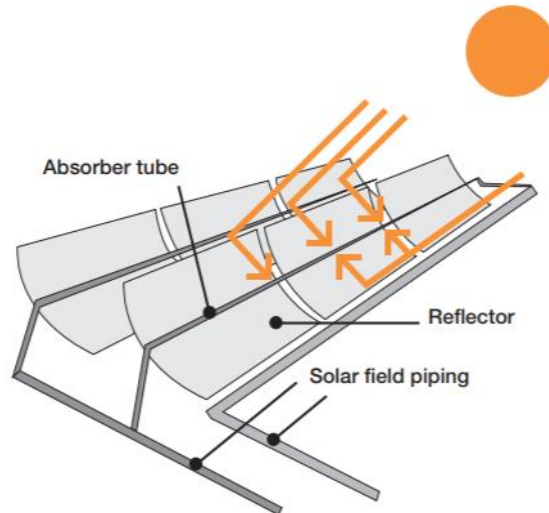


Figure 2.3 Diagram of Parabolic trough [16]

(ii) Central Receiver/Solar Tower

The receiver is mounted at the top of a tower and the sunlight concentration is done by a circular array of heliostats which are large individually-tracking mirrors. A heat transfer medium absorbs the highly concentrated radiation reflected by the heliostat and gets heated up. The absorbed heat energy is then used to generate superheated steam for turbine operation which then generates electricity [16]. Figure 2.4 gives an idea about the central receiver or solar tower.

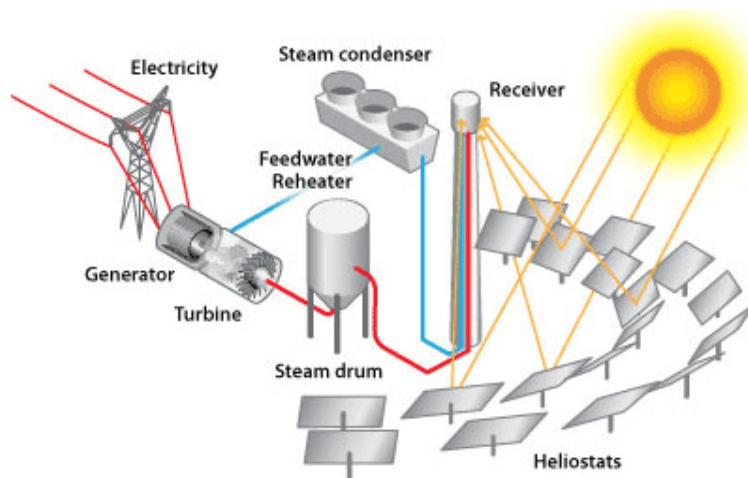


Figure 2.4 Diagram of Solar tower [16]

(iii) Parabolic dish

The sunlight is concentrated with the help of a parabolic dish-shaped reflector on a receiver placed at the focal point of the disc [16]. Only direct radiations that enters the system parallel to its optical axis are concentrated by the parabolic dish. Hence the solar dish has to be oriented always facing the sun. It requires two-axes tracking as it is a point-concentrating system. Since the concentration happens in the focus only the system temperature can reach up to 800° C. The high temperature allows a high thermal-mechanical energy conversion leading to higher solar-to-electricity efficiencies [17]. More than 30% efficiency solar-to-grid have been reached by the parabolic dish among concentrated solar power (CSP) systems [18].

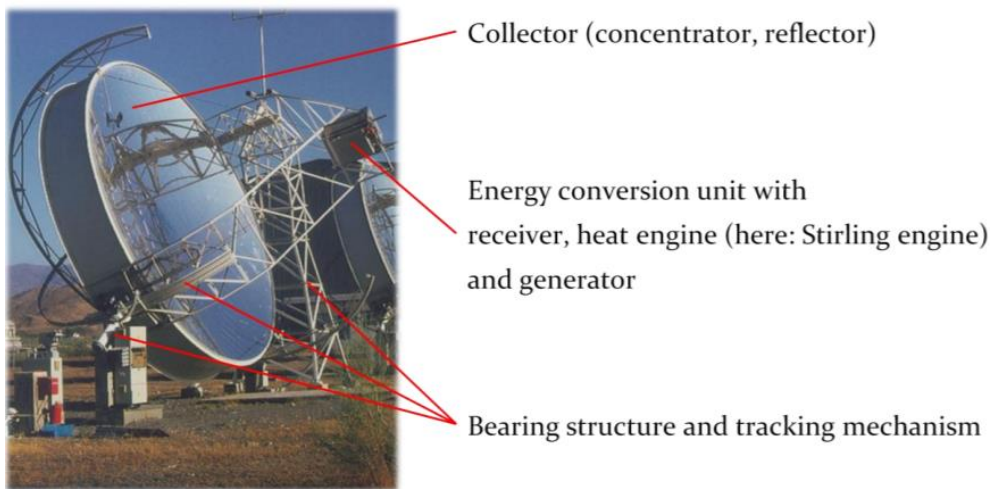


Figure 2.5 Components of Parabolic dish [18]

(iv) Linear Fresnel Collector:

Linear Fresnel Collectors, a subgroup of linear concentrating collectors use linear receivers and reflectors. The linear receivers are segmented in single axis tracking heliostat and are typically aligned horizontally to track the sun so that the receiver is illuminated without the need of moving the whole system. Figure 2.6 shows a diagram of linear Fresnel collector [19].

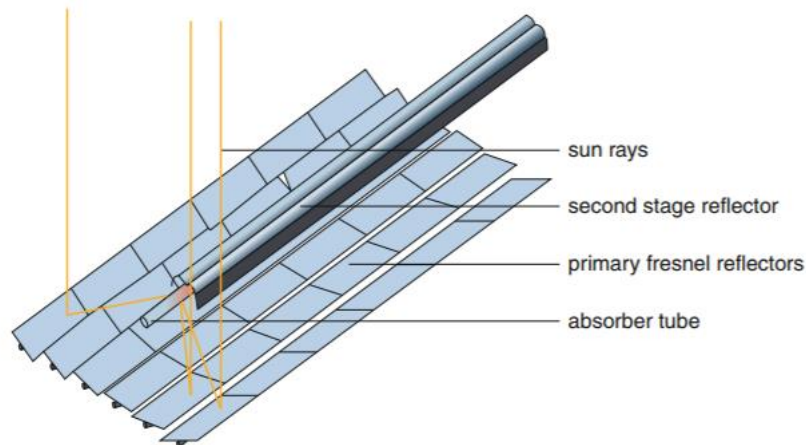


Figure 2.6 Diagram of linear Fresnel collector [19]

Linear Fresnel collector allows a bigger aperture area per unit of receiver compared to an ideal reflector (parabolic trough). The most amazing fact about the heliostat systems is that the aperture size of a complete system is independent of the size of the individual reflectors. Therefore, the individual reflectors can either be small or big but jointly will be able to cover a big aperture area. However, the heliostat systems have a drawback which is, it has a lower optical efficiency per reflector area due to the interference between individual reflector segments [19].

2.1.2.2. Compound Parabolic Collector (CPC)

Compound parabolic collectors belong to non-imaging concentrating collectors. These systems comprise of two parabolic reflectors with different focal points. Hence the nomenclature compound parabolic collector. Figure 2.7 shows the basic shape of the collector. Tracking systems are not required to operate these collectors which minimises the risk of mechanical failures and control mechanisms. However, the collector must be oriented in the right direction towards south (if mounted in the northern hemisphere and vice versa) in order to obtain maximum result.

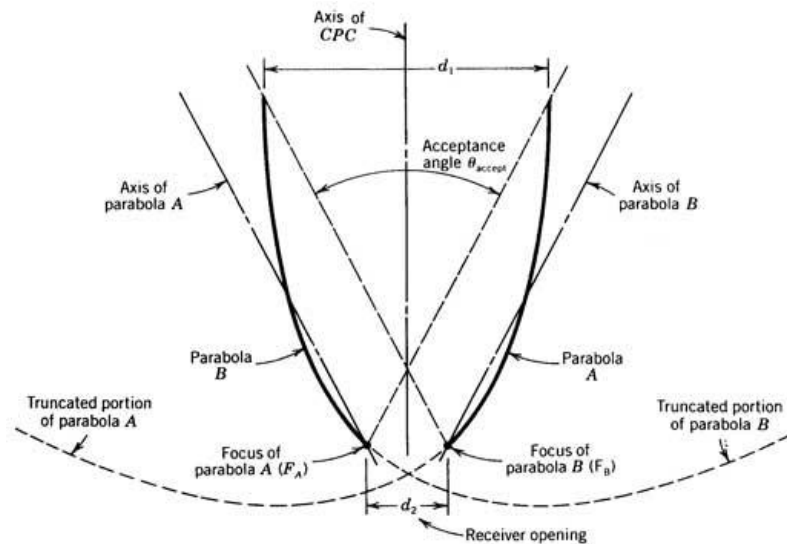


Figure 2.7 Compound Parabolic Collector [21]

The 'receiver opening' in the bottom is the distance between the focuses of the two parabolas A and B. It is where the receiver is placed. Both the parabolas reflect the incoming solar radiation onto the receiver. On each parabola lies the focal point of the other parabola. Moreover, symmetry exist between the focal point and the axis of the compound parabolic collector. The acceptance angle between the parabolas determines the amount of light that can be reflected and finally end up on the receiver. The interesting fact is, if an incident ray happens to be in the range of the acceptance angle, it will definitely be reflected by either of the parabolic reflectors and reach the receiver. The same principle applies for those rays falling outside the range of the acceptance angle. The rays falling outside the acceptance angle will be reflected from parabolic reflectors however not to the receiver instead reflected back outside the collector [20].

2.1.2.3. Maximum Reflector Collector (MaReCo):

The MaReCo or Maximum Reflector Collector is an asymmetrical truncated trough-like CPC collector. It is mainly designed for higher latitude usage. It is a non-tracking collector with bi-facial absorber. The usage of bi-facial absorber helps minimize the absorber area hence reducing the cost of production. It has a versatile usage ranging from stand-alone mounting on ground to the roof top integration [15].

Compared to the expensive PV and thermal absorbers, the reduction in the collector area in the concentrating collectors allows usage of cheap reflectors replacing the costly absorbers hence reducing the cost. The solar input for PV cells are increased due to the concentrating factor of the solar irradiance by the collectors. However, the increase in the solar irradiance results in an increase in cell temperature leading to decrease in PV cell efficiency. Circulation of running cooling water removes the built up high temperature. The warm water now can be used as an additional application, either heating up space or simply supplying warm water to the house. Thus, the hybrid concentrating collectors provide an advantage of collecting both thermal and electrical energy from the same collector.

The advantages of Maximum Reflector Collector (MaReCo) compared to PV and solar thermal collectors are

- Increase of the cell efficiency due to the reduction of cell operating temperature from the circulating cooling water. It is very essential in Photovoltaic and thermal hybrid (PV-T) collectors to remove heat from the receiver to cool down the cells efficiently and evenly.
- Lower production cost of a unit of PV-T due to the usage of fewer raw materials compared to an equivalent area of thermal and photovoltaic panel. As a result, this enables a lower production cost per kWh of annual produced heat and electricity.
- Deployment of more installed capacity per area because of the reduction of installation area allowing a lower installation cost [21].
- Longer lifetime of PV cells.

2.1.2.3.1. Structure of MaReCo:

A basic structure of a CPC trough is showed in Figure 2.8. The reflector consist of three parts-

Part A: the upper parabolic reflector between points 2 and 3. Its reflection focuses on the top of the absorber.

Part B: a circular part between points 1 and 2. This part transfers the light onto the absorber. The main significance of this part is that the lower tip of the absorber can be placed anywhere between the point 1 and point 2.

Part C: the lower parabolic part between point 4 and point 1

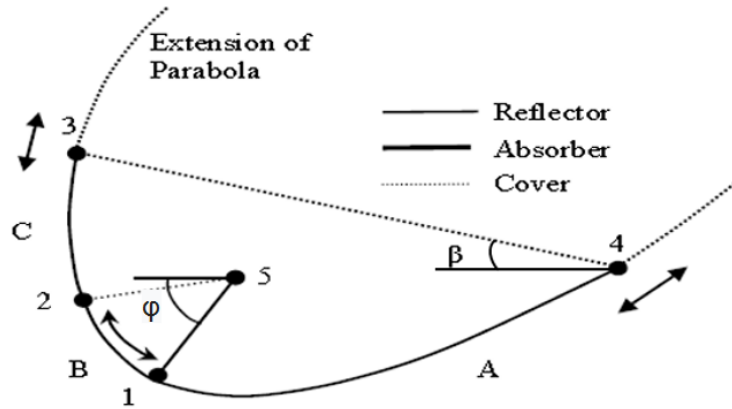


Figure 2.8 Basic structure of MaReCo [15]

φ is the aperture tilt angle and β is the absorber inclination angle. The cover glass is attached between points 3 and 4. The position of the cover glass depends on the position of the reflector along the extended parabolas where maximum annual irradiation onto the aperture is obtained [15].

2.1.2.3.2. MaReCo prototypes:

- (i) The stand-alone MaReCo

The stand-alone MaReCo has a cover glass tilt of 30° (for Stockholm conditions) with respect to the horizontal. The upper acceptance angle is 65° and the lower acceptance angle is 20° . It has a concentration area of $C_i = 2.2$. A diagram of the stand-alone MaReCo is shown in Figure 2.9. The collector is mainly designed as a stand-alone collector stationed in large empty fields which is then connected to a district heating system.

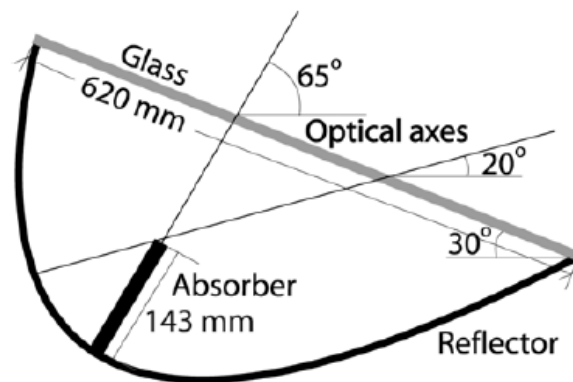


Figure 2.9 Diagram of stand-alone MaReCo (for Stockholm conditions with cover glass angle of 30°) [15]

- (ii) The roof integrated MaReCo

As already the name suggests, the roof integrated MaReCo are specially designed for mounting on the roofs. The difference between roof integrated and stand-alone MaReCo is that, the roof integrated MaReCo has a smaller depth in order to fit on the roof connecting to a heating system in a building. Here the cover glass starts where the circular part of MaReCo ends which means the glass is between points 2 and 4 in Figure 2.8. Hence, there is no upper parabolic reflector and so the absorber is placed

right beneath the cover. Since this collector is mounted on the roof of a building, it is tilted as the roof angle. All radiations ranging from 0° to 60° angle of incidence from the glass cover normal is accepted by the reflector. The angle 60° is determined by the roof angle and the reflector accepts radiation from the horizon to the normal of the glass. The collector functions like a flat plate collector above the angle 60° with an absorber area of $1/3^{\text{rd}}$ of the aperture area which is the front side of the absorber. It has a concentration area of C_i 1.5 when the roof is tilted at 30° with respect to the horizon. A diagram of roof integrated MaReCo is shown in the Figure 2.10.

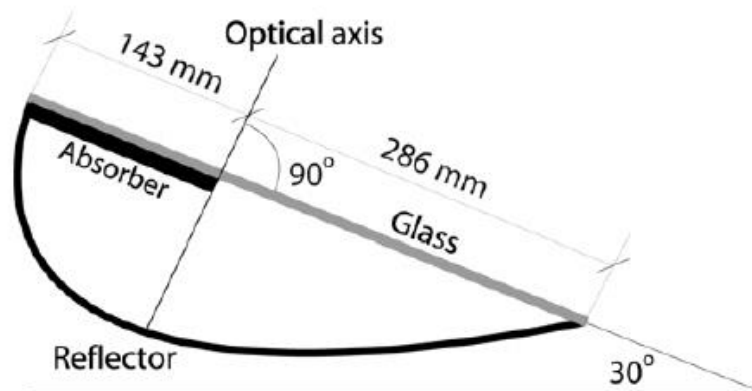


Figure 2.10 Diagram of roof integrated MaReCo [15]

(iii) The east/west MaReCo

This type of MaReCo is designed for exceptional cases when the roofs are not aligned in the east/west direction. In this case the reflector axes is aligned in the east/west direction that is, it is tilted along the roof. Radiations in the range of 20° to 90° are accepted from the cover glass normal as seen in the Figure 2.11. This collector comes with a concentration area of 2.0

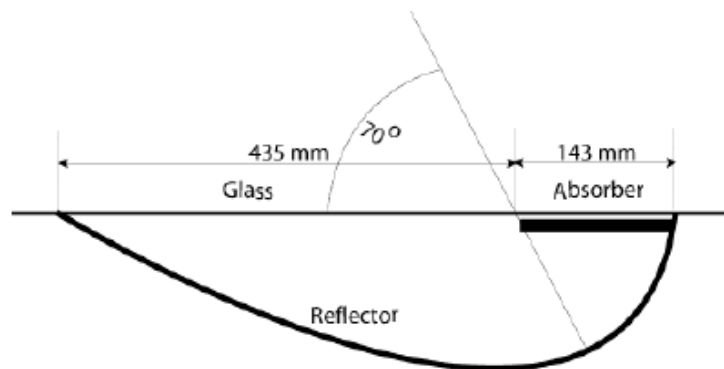


Figure 2.11 Diagram of east/west MaReCo with 70° optical axis from the cover glass [15]

(iv) The spring/fall MaReCo

The main objective behind this MaReCo prototype is to have a high solar fraction in the heating system over the whole year. The geometry is designed such that it enables to maximise its efficiency during spring and fall when the heating demand is high and low efficiency during summer when the heat demand is less preventing over-heating the system. Radiations lesser than the angle 15° will be reflected back

outside the collector. Here the absorber is placed just below the cover glass. The spring/fall MaReCo has a concentration area of $C_i = 1.8$. Figure 2.12 shows a diagram of spring/fall MaReCo.

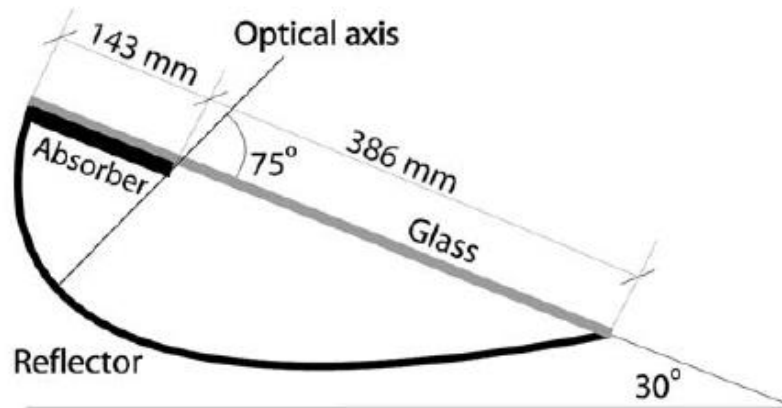


Figure 2.12 Diagram of spring/fall MaReCo for roof tilt 30° [15]

(v) The wall MaReCo:

An alternative to the east/west MaReCo or the spring/fall MaReCo is the wall MaReCo. It is a collector which can be mounted on a wall. Considering both sides of the absorber, concentration area is $C_i = 2.2$. The range of acceptance angle is from 25° to 90° from the horizon. The absorber is also placed just below the cover glass. Figure 2.13 shows a diagram of the wall MaReCo.

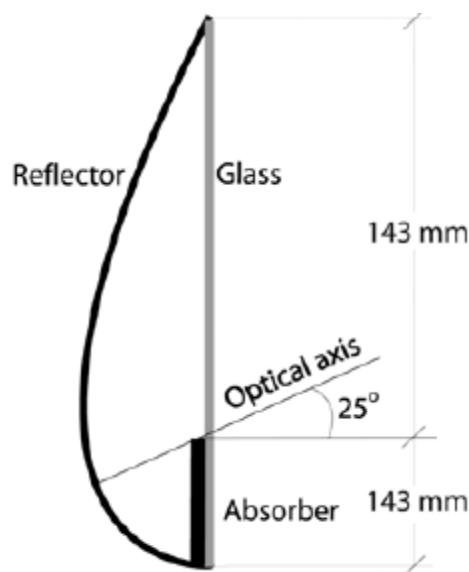


Figure 2.13 Diagram of wall MaReCo designed for south facing with optical axis at 25° from the horizon [15]

2.2. Solarus PowerCollector:

PowerCollector compound parabolic collector developed and marketed by Solarus. The design is similar to the roof integrated MaReCo. Solarus' PowerCollector comprises of two types of collector, a hybrid concentrated photovoltaic (C-PVT) and a thermal (C-T) collector. The geometry of the receiver concentrating the sunlight is a patented Maximum Reflector Collector (MaReCo) technology. An

aluminium reflector is used as the concentrator. The receivers are designed such that an aluminium thermal absorbers is being sandwich between two PV modules. The upper side of the receiver absorbs direct sunlight and the back side receiver collects the reflected and concentrated solar energy. These PowerCollectors perform very well even in cloudy conditions due to its optimised mirror technology which make it different from any other concentrators. It has a low concentration ratio, therefore performs great in stationary non-tracking mode. Hence cutting down the complexity of the system and the maintenance.

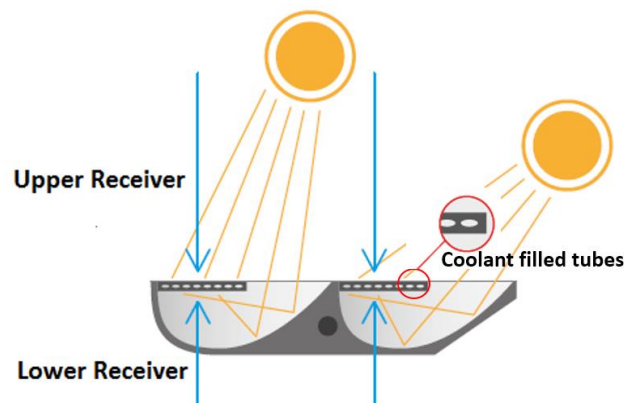


Figure 2.14 Solarus PowerCollector showing the upper and lower receiver [22]

PV cells do not go well with heat. For every 10° C rise in temperature, their electrical output decreases by 5%. The very efficient aluminium receiver and the Active Cell Cooling (ACC) plays a huge role in keeping the PV cells in good conditions with respect to heat. Solarus uses silicon instead of EVA which enables the Solarus PowerCollector to operate at temperature above 80° C without any material problems [22].

2.2.1. C-PVT

The hybrid concentrated photovoltaic produces both electricity and heat. Figure 2.15a and 2.15b gives an idea of the actual collector from Solarus.



Figure 2.15a PowerCollector C-PVT side view [22]



Figure 2.15b PowerCollector C-PVT silver [11]

PowerCollector C-PVT has two versions of products from Solarus which are C-PVT Black and C-PVT Silver. The C-PVT black is used for in roof installations. The only difference in the specifications between them is C-PVT black produces $1350 W_{th} + 270 W_{el}$ and C-PVT silver $1250 W_{th} + 270 W_{el}$.

2.2.2. C-T

The PowerCollector C-T produces only heat either to heat up space or water. A picture of C-T is shown in figure 2.16. The power specification of the PowerCollector C-T is $1500W_{th}$. The collector also has an aluminium receiver but it does not come with Active Cell Cooling (ACC).



Figure 2.16 PowerCollector C-T [11]

3. Numerical study method:

The Solarus PowerCollectors are based on the roof integrated MaReCo. An extensive simulation is done with the roof integrated MaReCo at Lisbon which serves as the baseline for the other experimental model simulations. The power output and the number of photons collected on the receiver of the solar collector is analysed in details with respect to the time of the year, the inclination angle of the collector and also the hourly variation of the day. Firstly, to check the feasibility of the already designed and available Solarus PowerCollector in the market, simulations are performed at three different locations Lisbon, Gävle and Delhi. Changes are made with the orientation of the collector to analyse further improvement in the output of the collector. Secondly, the roof integrated MaReCo is redesigned with the receiver position shifted towards the middle section of the aperture. Comparisons are made between the collector models.

The market and solar energy potential is much higher in the equatorial regions. Parabolic collectors are designed for such regions due the symmetrical positioning of the sun. Two solar collector models - parabolic collector with receiver at side edge and parabolic collector with horizontal receiver at the focus are designed and simulated at Nairobi (1.2921° S, 36.8219° E) and at Lisbon. The results are compared afterwards with each other.

The construction of the simulation structures and all the simulations are being performed in the solar ray tracing software Tonatiuh. The output of the software is processed as binary data file. An additional software called Mathematica is used to post process the binary data file output and determine what the work requires.

3.1. Collector Simulations

Tonatiuh is used for designing and simulation of the solar concentration collector. The post procession is performed with the help of Mathematica. The description of the two softwares are given in section 3.1.1 and 3.1.2.

3.1.1. Tonatiuh Program

“Tonatiuh is an open source advanced object oriented Monte Carlo ray tracing program which assists in the designing and analysis of solar concentrating systems” [23]. The program is designed, developed, implemented, verified and validated by the Department of Engineering of The University of Texas supported by the Department of Energy (DOE) and National Renewable Energy Laboratory (NREL) under the Minority Research Associate (MURA) subcontract [23]. The Tonatiuh logo is shown in figure 3.1.



Figure 3.1 Tonatiuh logo [24]

The program is written in C++. Hence, using, maintaining and extending is an easy task [25]. The program can be used in Windows, Mac and Linux. Within the software the computational scheme provided are as below-

- (i) A concentrating system model
- (ii) An incoming solar radiation model
- (iii) A model of the basic interactions between the radiation and the elements of the concentrating system, and
- (iv) A flexible output format to choose from the program as per the user's requirements

Tonatiuh comes with various feature. Some of the most relevant are-

- The software is based on a powerful theoretical foundation for the optical simulation of almost any solar concentrating systems
- An architecture of the software so clean and flexible which allows the users to adapt, expand, increase and modify its functionalities with minimum effort.
- Independence of the operating system at source level, it runs with Windows, Mac and Linux.
- The software is equipped with an advanced easy-of-use Graphic User Interface (GUI) [23]

Before running the Tonatiuh simulation, the user can choose from the three options how the output information can be saved-

- Not export:

Tonatiuh will not save any ray tracing simulation results if selected this option. The main purpose of this option would be to test the accuracy in the model of the optical system before it is actually being exposed to a large number of rays.

- Binary data files:

If selected this option, the Tonatiuh software is being instructed to save the output as binary data files. Depending on the types of the information of the photons saved, the format for the binary files varies accordingly. A summary of the saved binary information is depicted in as associated ASCII file.

- SQL Database:

If selected this option, instructions are given to the Tonatiuh software to save the ray tracing results in a SQL Database. To store different fragments of information, different database's tables are used-

- (a) Surfaces: stores the basic identification information of the surfaces the photons are intersecting.
- (b) Photons: stores the intersection-related information of each photon intersecting the concentrating geometry
- (c) WPhoton: stores the power associated to each photon [26].

3.1.2. Mathematica Program

Mathematica also termed as Wolfram Mathematica is mathematical computation program used in scientific, engineering and computing work places. The brainchild behind Mathematica is Stephen Wolfram however, the program was developed by Wolfram Research of Champaign, Illinois. The programming language used in Mathematica is Wolfram Language [27]. The Wolfram logo is shown in figure 3.2.



Figure 3.2 Wolfram Mathematica logo [27]

3.2. Design of the MaReCo structure with Tonatiuh

Maximum Reflector Collector or MaReCo is an asymmetric trough-shaped compound parabolic collector. The basic structure of MaReCo is a combination of an upper parabolic part, a lower parabolic part and a circular section in between. Many MaReCo prototypes exist however, the roof integrated MaReCo is mainly used in the thesis work. Some variations are also made on the roof integrated MaReCo design to analyse its performance and compare it with the initial design.

3.2.1. Design of roof integrated MaReCo

3.2.1.1. Structure of the collector

The structure of a roof integrated MaReCo is different from the usual MaReCo structure. The cover glass starts from the starting of the circular section till the lower parabolic part. There is no upper parabolic section.

Therefore, a cylindrical shape and a trough parabola are used to design the model. Figure 3.3 shows the roof integrated model made with Tonatiuh.

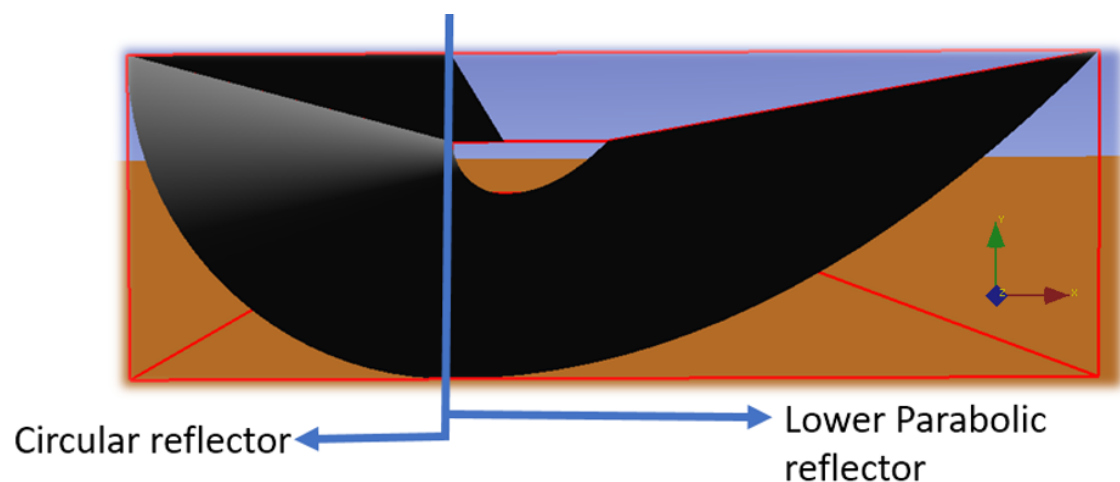


Figure 3.3 Roof integrated MaReCo showing the circular reflector and the lower parabolic reflector

The centre of the circular section of the cylinder is made to coincide with the focus of the parabolic trough. The radius of the circular section of the cylinder is 143mm, same as the length of the receiver. The optical axis of the parabolic trough is right angled to the receiver. The length of the opening aperture is 286 mm. The focus of the parabolic trough is made the same as the radius of the cylindrical section in order to make the centre of the circle and the focus of the parabola coincide (side view). The total length of the collector in the transverse side is 2310 mm. The receiver is placed at the starting of the cylindrical section with the same length 2310 mm. Figure 3.4 shows a roof integrated MaReCo with the mentioned dimensions.

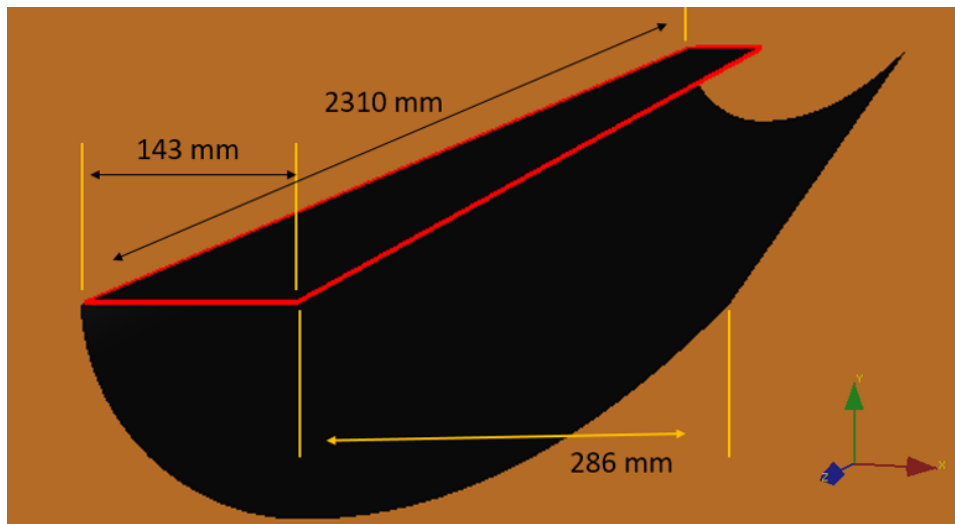


Figure 3.4 Roof integrated MaReCo with dimensions

As for the type of material, specular standard material option is used for all the shapes chosen to model the MaReCo structure. For ideal case the reflectivity of the cylindrical structure and the parabolic trough are kept at 1. The reflectivity of the receiver is always kept 0.

3.2.1.2. Orientation of the collector

In the northern hemisphere, to maximise the output, the solar panel are usually aligned in the east-west direction facing south because of the position of the sun. The opposite vice versa happens when the solar panel needs to be fixed in the southern hemisphere. Figure 3.4 shows a solar panel fixed facing south in Los Angeles (latitude 34° N).

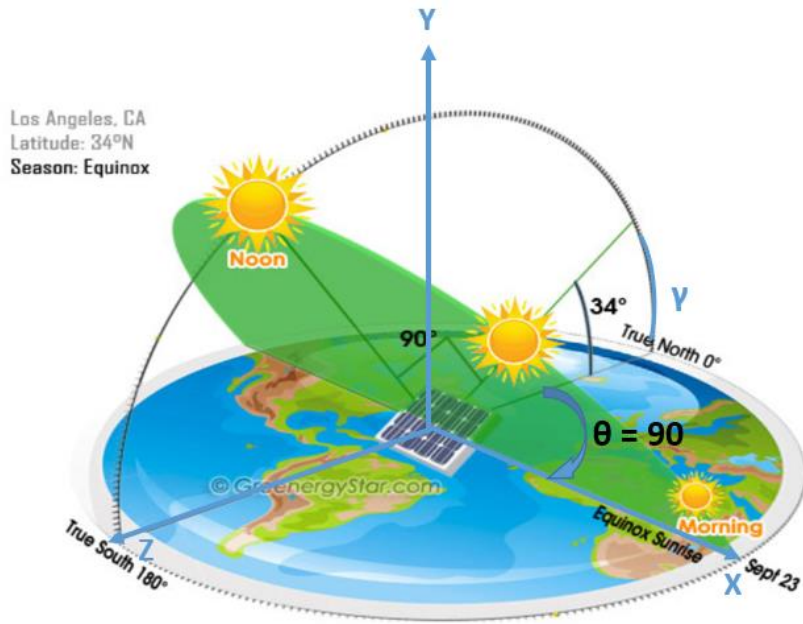


Figure 3.5 Diagram of a solar panel in Los Angeles (latitude: 34° N) facing south [29]

Tonatiuh by default do not fix the position of the design model towards the east-west direction. By default the model in Tonatiuh is facing towards the west. Therefore, the model has been made to rotate right angle towards south. The simulations are done with various tilt angles, hence the solar concentrator model has been tilted in angles ranging from 0° to 65°. The model has been made to rotate two times. This orientation of the solar collector model is performed in Tonatiuh with the help of quaternion rotation. A quaternion has four variables x, y, z and w [30]. Since the model is rotated in two different axis, a quaternion multiplication is performed to find the new quaternion variables.

Since the model is rotated along the y-axis for the east-west alignment and then the z-axis for the tilt, $n(q)$ and $n(r)$ are defined as-

$$n(q) = (0 \ 1 \ 0) \quad (5)$$

$$n(r) = (0 \ 0 \ 1) \quad (6)$$

$\theta = 90^\circ$, where θ is the angle rotated to align the collector in east-west direction

$\gamma = \text{tilt angle}$, γ ranges from 0° to 65°

'q' and 'r' are individual vector representing each plane and 't' is the cross product of them. The equation of each vectors are given below-

$$q = q_0 + iq_1 + jq_2 + kq_3 \quad (7)$$

$$r = r_0 + ir_1 + jr_2 + kr_3 \quad (8)$$

'q' and 'r' are calculated according to the equation below-

$$q = (\cos \frac{\theta}{2}, \hat{n} \sin \frac{\theta}{2}) \cdot n(q) \quad (9)$$

$$r = (\cos \frac{\gamma}{2}, \hat{n} \sin \frac{\gamma}{2}).n(r) \quad (10)$$

$$t = q \times r \quad (11)$$

$$t = t_0 + it_1 + jt_2 + kt_3 \quad (12)$$

Where,

$$t_0 = r_0q_0 - r_1q_1 - r_2q_2 - r_3q_3 \quad (13)$$

$$t_1 = r_0q_1 + r_1q_0 - r_2q_3 - r_3q_2 \quad (14)$$

$$t_3 = r_0q_2 - r_1q_3 - r_2q_0 - r_3q_1 \quad (15)$$

$$t_4 = r_0q_3 - r_1q_2 - r_2q_1 - r_3q_0 \quad (16)$$

Finally the x, y, z, w values of the quaternion is calculated by-

$$w = rad[2 * (\cos^{-1} t_0)] \quad (17)$$

$$x = \frac{t_1}{\sin \frac{[2 * (\cos^{-1} t_0)]}{2}} \quad (18)$$

$$y = \frac{t_2}{\sin \frac{[2 * (\cos^{-1} t_0)]}{2}} \quad (19)$$

$$z = \frac{t_3}{\sin \frac{[2 * (\cos^{-1} t_0)]}{2}} \quad (20)$$

3.2.1.3. Time structure

The default settings in Tonatiuh regarding the time settings is in two ways, UT (Universal Time) and CT (Central Time). The time given in the UT section is based on the Universal standard timing. Therefore, for local time of a particular the required correction is performed. In this current work, corrections in timings are taken into correction with Lisbon (+1), Gävle (+2), Delhi (+5.30) and Nairobi (+3).

3.2.1.4. Solar rays

The average value of the irradiance which is 1000W/m² of the sun is taken as the fixed value throughout the simulations. The position of the sun changes as per the locations where the collector is simulated.

The simulation is done with 75000000 number of rays. The output of the simulation is saved in binary data files. Hence, all the photon information is stored in terms of binary code. The information is then post processed and extracted with the help of Mathematica. Finally, the desired results are being calculated with the help of Mathematica.

3.2.2. Design of modified MaReCo models

A new model is made by shifting the position of the receiver. In the new model the receiver is placed right in the middle of the intersection plane between the cylindrical section and the parabolic trough. A figure of the new modified model is shown in Figure 3.5.

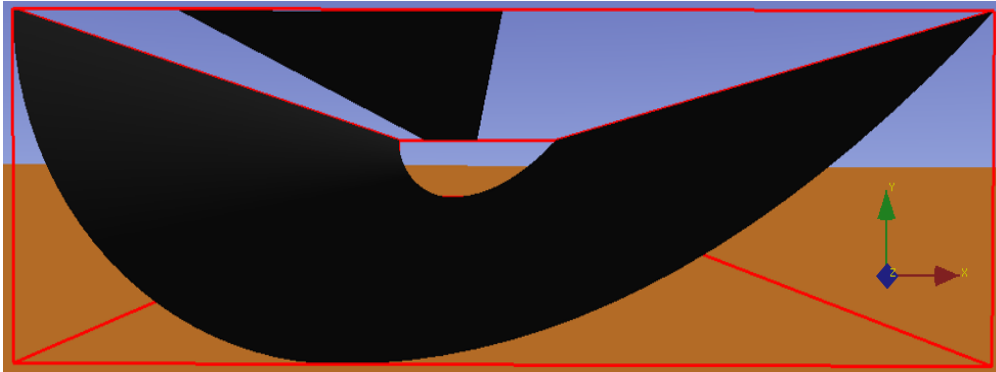


Figure 3.6 Modified model of the roof integrated MaReCo

3.2.3. Design of Parabolic collector with receiver at the side edge

Symmetrical collectors can be a huge potential near the equatorial regions. The design itself is simple and less complicated. The aperture opening and the dimension of the receiver is kept the same as the MaReCo to ensure similar conditions to compare and keeping the price factor at check. Similar to the roof integrated design the receiver is positioned at the side edge.

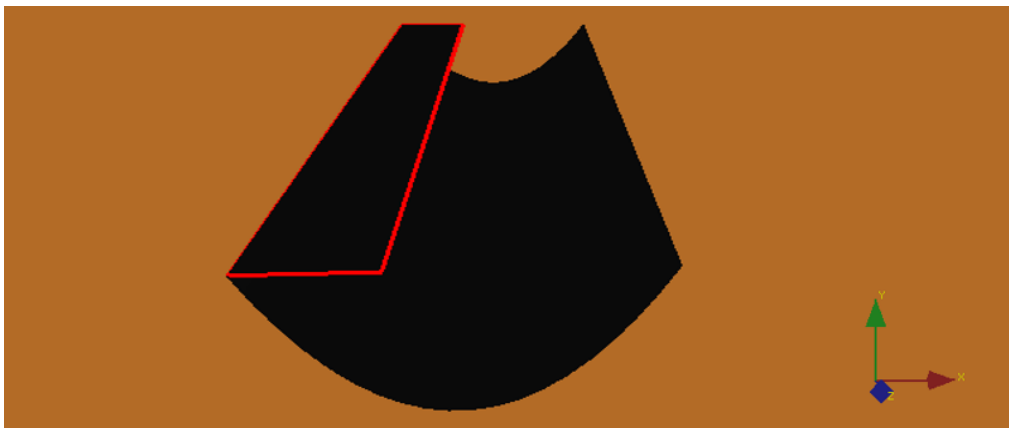


Figure 3.7 Parabolic collector with receiver at side edge

3.2.4. Design of parabolic collector with horizontal receiver at the focus

The position of the receiver is the same in this model. Only one receiver is used with a different orientation. The receiver is rotated at right angle to make it horizontal with respect to the ground when the solar collector is in zero inclination. The active part of the receiver is set at back since the interest in knowing the amount of photons received on the back is more rather than the front.

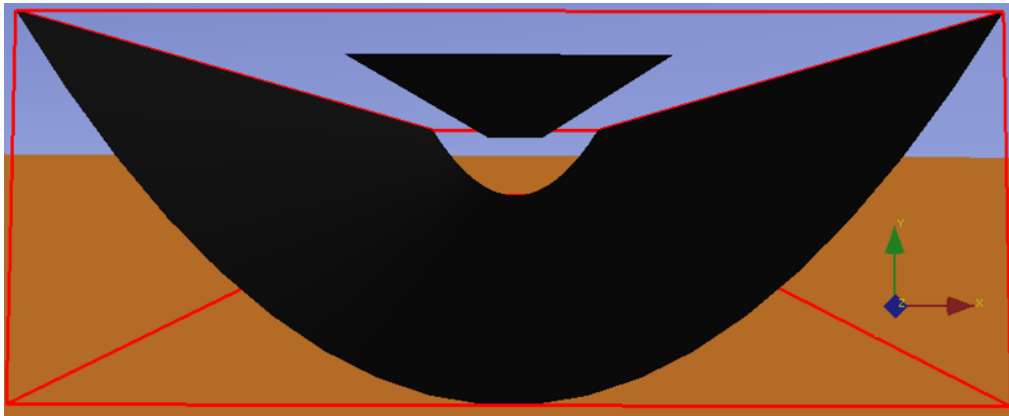


Figure 3.8 Parabolic collector with horizontal receiver at the focus

3.3. Post processing with Mathematica

The Tonatiuh outputs are saved as dat files and an ASCII file with a summary of the information stored inside the dat files. Each ASCII file of each simulation output starts with the string “START PARAMETER” and ends with “END PARAMETER”. Between these two strings the parameters exported for each photon are being recorded. Each line between the strings are used to defined each parameters exported which is the information about one surface that is the identifier used for the surface in binary files and the URL of that surface. The next line after that gives an information related to the surface. At the end, the last line in the ASCII file gives the power per photon in watts which is to be considered when calculating solar fluxes or power values. Figure 3.9 shows an example of an ASCII file. The file is taken from the simulation done with the roof integrated MaReCo in Lisbon on March 20th. The inclination of the MaReCo is 5° with respect to the horizontal [26].

```

_parameters - Notepad
File Edit Format View Help
START PARAMETERS
id
x
y
z
side
END PARAMETERS
START SURFACES
1 //SunNode/RootNode/ConcentratingSurface/Receiver/TShapeKit1
END SURFACES
1.95379e-05
  
```

Annotations in the image:

- A bracket on the right side of the parameters (id, x, y, z, side) is labeled "5 parameters".
- An arrow points from the text "1 surface" to the line "1 //SunNode/RootNode/ConcentratingSurface/Receiver/TShapeKit1".
- An arrow points from the text "1 power per photon" to the value "1.95379e-05".

Figure 3.9 Information inside an ASCII file

In this particular case 19 binary files were obtained, each of them containing in the order of 10 million of 5-tuples. Each 5-tuple provide the following information about a photon falling on the flat receiver:

- The photon id
- The x-coordinate of the photon
- The y-coordinate of the photon
- The z-coordinate of the photon

- The side of the surface in which the photon is impinging [28]

Moreover, since there is only one line between “START SURFACES” and “END SURFACES” the ASCII files also displays that only photons related with one surface have been stored.

A set of instructions or codes are given to Mathematica in order to extract the information and process to obtain or result. Figure 3.10 shows the instruction given to Mathematica (same example has been taken, 20th March, Lisbon, 5° inclination).

```

In[45]:= SetDirectory[NotebookDirectory[]]
Out[45]= C:\Users\Seram\Desktop\Simulations\lisbon_12

In[46]:= side[{photonID_, x_, y_, z_, sideID_}, refSide_] := sideID = refSide

In[47]:= file = FileNames["*.dat"]
Out[47]= {_10.dat, _11.dat, _12.dat, _13.dat, _14.dat, _15.dat, _16.dat, _17.dat, _18.dat,
_19.dat, _1.dat, _2.dat, _3.dat, _4.dat, _5.dat, _6.dat, _7.dat, _8.dat, _9.dat}

numberOfFiles = Length[file]

In[54]= 19
Out[54]= 19

In[55]:= totalNumberOfPhotons = 0
Out[55]= 0

In[49]:= powerPerPhoton = 0.0000195379
Out[49]= 0.0000195379

In[50]:= For[i = 1, i ≤ numberOfFiles, ++i, fileRawData = BinaryReadList[file[[i]], "Real64", ByteOrdering → +1];
filePhotonSet = Partition[fileRawData[[1 ;; Length[fileRawData]]], 5];
Clear[fileRawData];
fileValidPhoton = Select[filePhotonSet, side[#, 0] &] /. {photonID_, x_, y_, z_, sideID_} → {x, z};
Clear[filePhotonSet];
fileNumberOfValidPhotons = Length[fileValidPhoton];
totalNumberOfPhotons = totalNumberOfPhotons + fileNumberOfValidPhotons;
totalNumberOfPhotons
]

```

Figure 3.10 Mathematica code

The first instruction tells Mathematica where to look for Tonatiuh’s results data files. The Mathematica file need to be saved in the same folder as the Tonatiuh’s data files are.

The second instruction is an auxiliary function which allows the software to determine if a photon is impinging in the correct side of the receiver.

The power per photon which we obtained for the ASCII file is given to the software which will be used later to calculate the estimated power in the receiver.

The set of remaining coding is for the purpose of processing the binary data files. The ‘For loop’ runs from $i = 1$ to $i = \text{numberOfFiles}$ which makes sure the processing of all binary data file output by

Tonatiuh. The first thing done for each and every binary data file, is to read the file as a list of double numbers ('Real64'). Then the list of double numbers are stored in the variable named "fileRawData". The following Mathematica statement performs this action.

```
fileRawData = BinaryReadList[file[[i]], "Real64", ByteOrdering -> +1];
```

From the ASCII file, every photon from the Tonatiuh output contains five vital information which are PhotonID, the three local coordinates, and the SideID indicating if the photon is impinging on the front or the back of the receiver. The next step is structuring the list of double numbers stored in the data file into raw list of numbers of these 5-tuples. The next Mathematica statement fulfils this command storing the newly created structured list of 5-tuples in the variable named "filePhotonSet".

```
filePhotonSet = Partition[fileRawData[[1 ;; Length[fileRawData]]], 5];
```

The initial list of double numbers has been partitioned into 5-tuples as "filePhotonSet". Hence, in order to save memory the content of "fileRawData" is being erase with the following Mathematica statement.

```
Clear[fileRawData];
```

The next Mathematica statement selects the only photons impinging on the back of the flat receiver facing towards the collector. Since the y-coordinate of the photons, the coordinates normal to receiver plane are unnecessary only the x and z coordinated are recorded. The 5-tuple information have been transformed into 2-tuple information and is stored in the variable named "fileValidPhoton" with the help of the next coding statement.

```
fileValidPhoton = Select[filePhotonSet, side[#, 0] &] /.  
  {photonID_, x_, y_, z_, sideID_} -> {x, z};
```

The contents of the "filePhotonSet" is no longer required. So to save up memory and space the variable is erased with the clear command.

```
Clear[filePhotonSet];
```

The total number of photons accumulated and recorded by the receiver is obtained by the following Mathematica statement.

```
fileNumberOfValidPhotons = Length[fileValidPhoton];  
totalNumberOfPhotons = totalNumberOfPhotons + fileNumberOfValidPhotons;
```

The total number of photons have been given an initial value of 0. With the help of the 'For loop', it is being constantly updated until the final value. Once the total number of photons are known, the estimated power in the receiver can be calculated with the next Mathematica statement [28].

```
estimatedPowerAtReceiver = powerPerPhoton * totalNumberOfPhotons / 1000 (* kW *)
```


4. Results and Discussions

Numerous simulations have been performed in various locations of the world, Lisbon, Gävle, Delhi and Nairobi with different solar collector models. Detailed comparative analysis of the cities with respect to each other in terms of the inclination angle of the collector, time of the year and time of the day is performed. More in-depth study about the feasibility and usability of the various collector models in different time of day at various time of the year have also been analysed. The section describes about the discussions regarding the obtained results.

4.1. Roof integrated MaReCo

4.1.1. Lisbon

Lisbon is located at the western part of Europe. The latitude and longitude of Lisbon is 38.7223 N and 9.1393 W.

4.1.1.1. Comparison of power with respect to tilt angle

Simulations are made in 21st June, 21st December, 20th March and 22nd September. The inclination angle is varied from 0° to 65° fixing the time of the day at local solar time 12.00. The MaReCo is facing south since the location is in the northern hemisphere. The location of the receiver is positioned in the upper part of the collector.

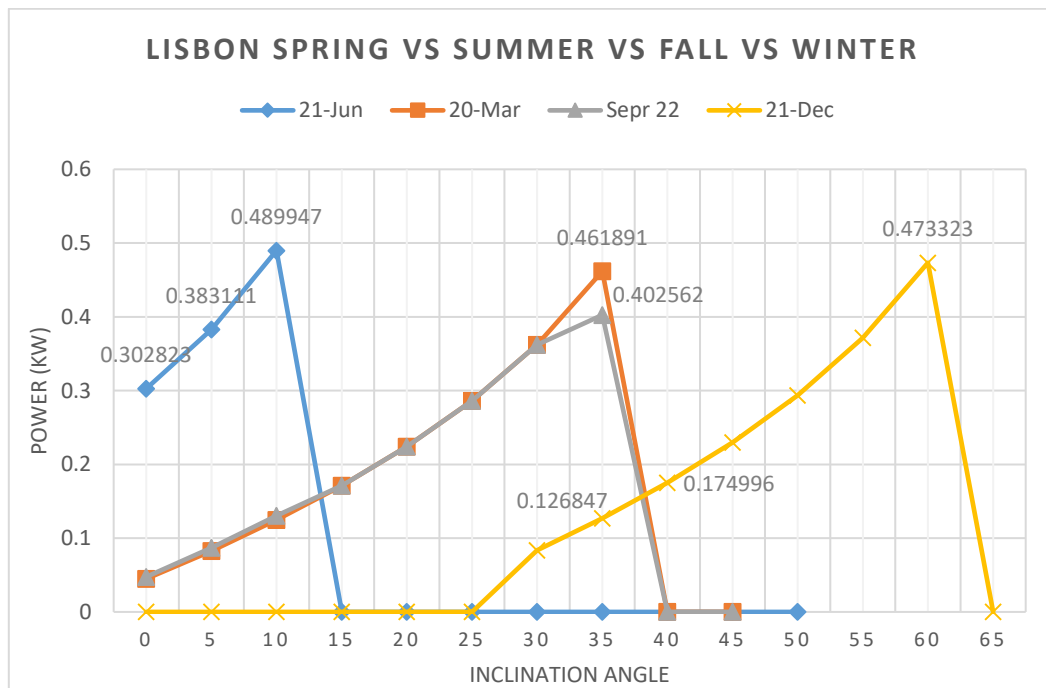


Figure 4.1 Comparison of the power during 21st June, 20th March, 22nd Sept and 21st Dec at the receiver in Lisbon at 12.00 with inclination angle of the collector ranging from 0° to 65°

The break-off point in summer, the angle after which collector stops producing power due to lack of solar radiation, is 10° with a maximum power output of 0.489947 kW. This is due to the reason that the sun is almost perpendicular to the solar collector since the elevation of the sun during summer is large.

Hence, most of the solar rays from the sun are reflected back with almost no rays reaching the receiver. An hourly simulation is performed at 10° inclination angle. The curve is shown in Figure 4.2

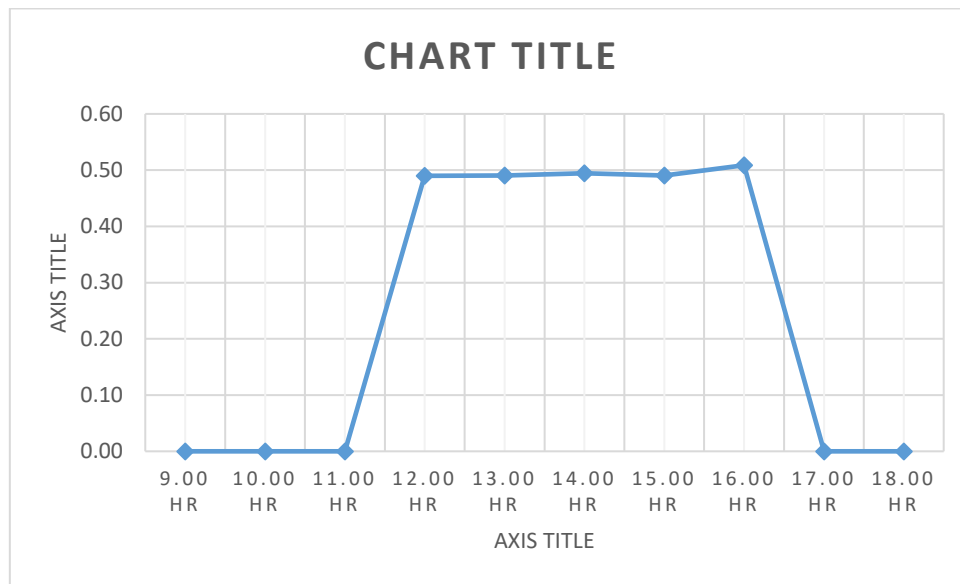


Figure 4.2 Hourly power production in Lisbon at June 21st with collector inclination angle 10°

The power production hours is limited from 11.00 till 17.00 in summer when the day is longest. This is due to the position of the sun with respect to the location.

The curve structure of March, September and December is approximately identical. The curve representing December is shifted more to the right since the power output starts from the collector inclination angle of 25°. The break-off angle of inclination of the collector is almost similar for spring and fall and the highest with winter. At the same time, the angle from which the collector starts receiving solar radiation and generate power in the receiver is also the highest with winter. This is due the reason of the position and the elevation of the sun in various season. In summer the elevation of the sun from the horizon is higher compared to the elevation of the sun in winter. And as usual for the fall and spring, the elevation of the sun lies in between summer and winter. The tilt angle of the MaReCo collector at which the receiver produces the maximum output from the Figure 4.1 is reproduced again in Table 1.

Table 1. The maximum power output tilt angle for spring, summer, fall and winter at Lisbon.

Location	Time	Day	Tilt angle	power at the receiver (kW)
Lisbon	12 hr	20-Mar	35	0.461891
Lisbon	12 hr	21-Jun	15	0.532858
Lisbon	12 hr	22-Sep	35	0.402562
Lisbon	12 hr	21-Dec	60	0.473323

The average roof angle of a house lies between 10° and 40°. Hence the roof integrated MaReCo structure is suitable for use during summer, spring and fall. However, for winter the output is very low. At an angle of 40°, the power output at the receiver is 0.174996 kW.

Table 2. Hourly power output at the receiver with 40° tilt angle of the solar collector in winter in Lisbon

Winter	Lisbon	40		
Location	Time	Day	Tilt angle	power at the receiver (kW)
Lisbon	9.00 hr	21-Dec	40	0
Lisbon	10.00 hr	21-Dec	40	0.051997
Lisbon	11.00 hr	21-Dec	40	0.119015
Lisbon	12.00 hr	21-Dec	40	0.174996
Lisbon	13.00 hr	21-Dec	40	0.209382
Lisbon	14.00 hr	21-Dec	40	0.213479
Lisbon	15.00 hr	21-Dec	40	0.182878
Lisbon	16.00 hr	21-Dec	40	0.129414
Lisbon	17.00 hr	21-Dec	40	0.063032
Lisbon	18.00 hr	21-Dec	40	0

The power output in winter at this inclination is very low compared to the other seasons. The maximum power output occurs at 14.00 with a value of 0.213479 kW. Due to shorter days the range of power output hour is very less, from 10.00 till 17.00

4.1.1.2. Orientation change of MaReCo

However, with a little orientation change in the solar collector, the output of the collector can be tremendously improved. The MaReCo is positioned in such a manner that, although it is still facing south the receiver is located at the bottom of the collector. The change in solar collector orientation is shown properly in Figure 4.3a and 4.3b.

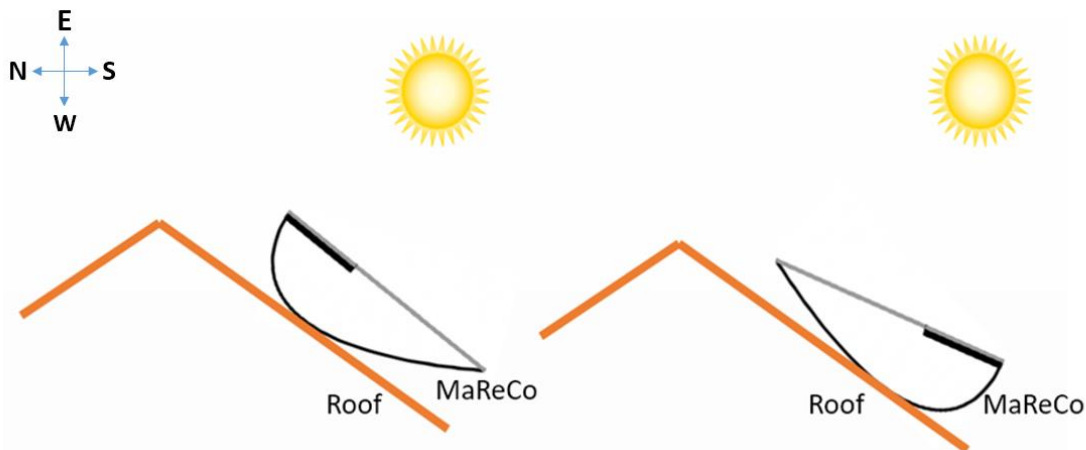


Figure 4.3a Normal orientation of MaReCo at Lisbon

Figure 4.3b Inverted orientation of MaReCo at Lisbon

Due to this new inverted orientation, more light rays enter the collector aperture producing more output power. With the same solar collector without any extra equipment or cost, with a little adjustment in the orientation, more output power can be achieved.

4.1.1.2.1. Inverted orientation in summer

Fixing the time of the day and varying the inclination angle of the solar collector, simulations are performed with the inverted orientation of the collector. The maximum power output is found to be 0.53286 kW at an inclination angle of 15° with the inverted orientation. The resulting graph is shown in Figure 4.4.

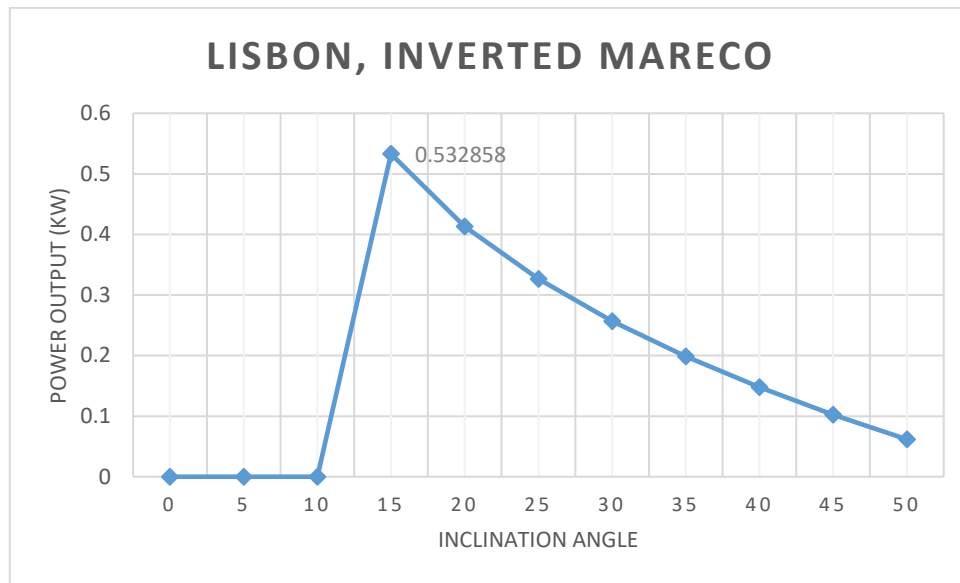


Figure 4.4. Power output (12.00 hour) vs inclination of the inverted MaReCo in Lisbon at June 21st

To check the feasibility of the inverted structure during the day, an hourly simulation in the maximum power output inclination angle which is 15° of the collector is performed in June 21st.

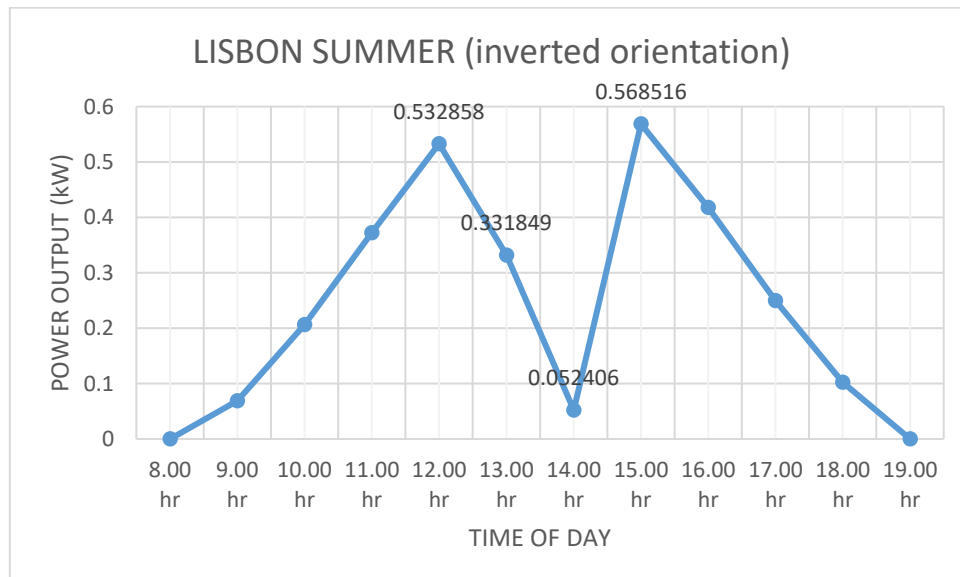


Figure 4.5 Hourly power output with fixed inclination angle at 15° (maximum power output angle) in Lisbon during 21st June

From the curve, a dip in pattern is seen from 12.00 until 15.00. This is the only disadvantage of the inverted collector orientation. This “cut-off” is due to the reason that during these hours the sun is directly

above the collector and majority of the rays are blocked by the receiver. The condition of solar rays entering through the side curve happens two times before and after the sun lies exactly above the solar collector. Although, the power production range has been improved from 11.00 to 17.00 in the normal orientation to 8.00 to 19.00 with the new orientation, the power output has been decreased in the peak hour of the day.

The curve shown in Figure 4.5 is represented again as a table to depict the number of photons received on the back side of the absorber.

Table 3 shows the hourly power received by the roof integrated MaReCo at Lisbon during 21st June from 9:00 to 18:00 hour. The power received is recorded as kW.

Summer	Lisbon	15		
Location	Time	Day	Tilt angle	power at the receiver(kW)
Lisbon	8.00 hr	21-Jun	15	0
Lisbon	9.00 hr	21-Jun	15	0.069182
Lisbon	10.00 hr	21-Jun	15	0.206326
Lisbon	11.00 hr	21-Jun	15	0.372494
Lisbon	12.00 hr	21-Jun	15	0.532858
Lisbon	13.00 hr	21-Jun	15	0.331849
Lisbon	14.00 hr	21-Jun	15	0.052406
Lisbon	15.00 hr	21-Jun	15	0.568516
Lisbon	16.00 hr	21-Jun	15	0.417694
Lisbon	17.00 hr	21-Jun	15	0.249995
Lisbon	18.00 hr	21-Jun	15	0.102550
Lisbon	19.00 hr	21-Jun	15	0.000135

4.1.1.2.2. Inverted orientation in spring, fall and winter

To check the performance of the inverted orientation of MaReCo during spring, fall and winter, simulations are performed at 20th March, 22nd September and 21st December.

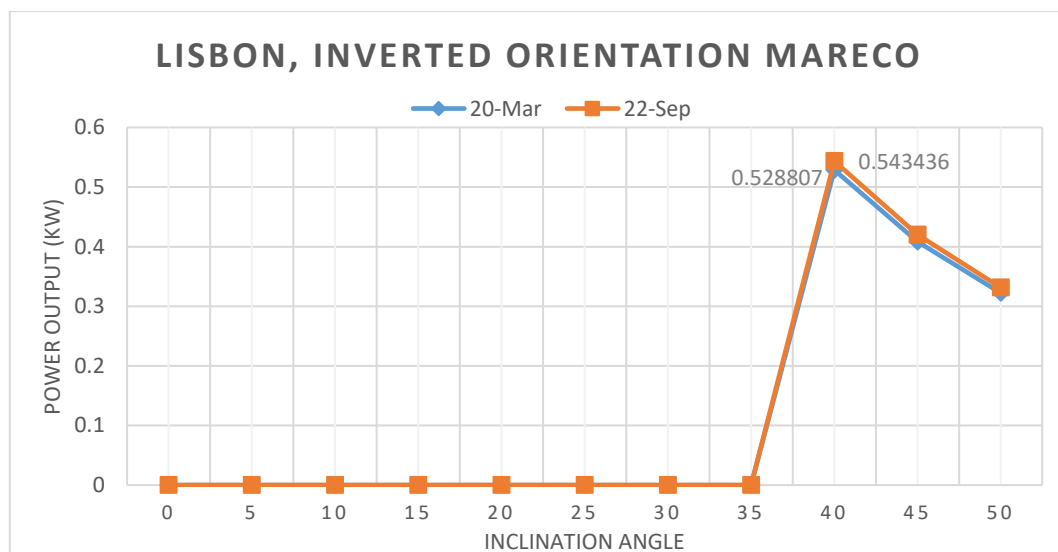


Figure 4.6 Power output (at 12.00) vs inclination angle in Lisbon during 22nd Sept and 20th March

From the curve, it is observed that the power output starts from 40° inclination with a high value of 0.528807 kW for March 20th and 0.543436 kW for 22nd September. The power output value is larger than the value obtained from the normal orientation. Hence, the inverted orientation is feasible for tilt angle 40° or greater. However, the work load for the maintenance is increased due to the change in the tilt angle of the collector from the 15° (peak power output for summer) to 40°. The inverted orientation does not produce any results during December. Hence, it is not suitable for winter.

4.1.1.3. Flux distribution at the receiver

The flux distribution of the solar radiation on the receiver on June 21st at the maximum output tilt angle, 15° of the collector is shown in Figure 4.7

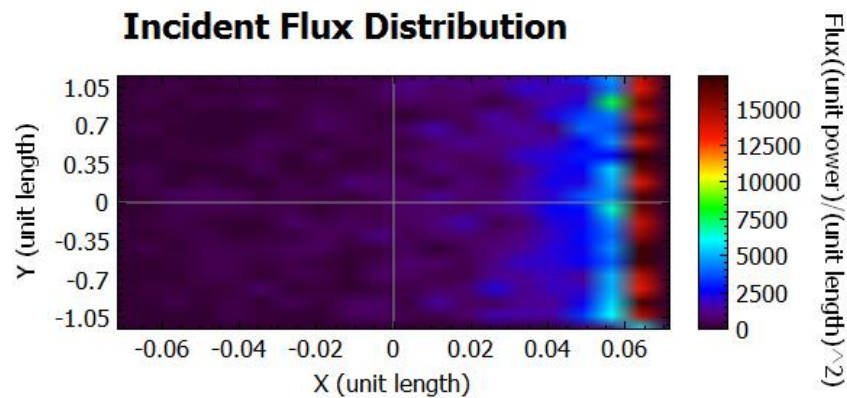


Figure 4.7 Flux distribution during summer at Lisbon

Most of the solar rays are received at the right end of the receiver. This is due to the reason that the focal plane of the parabolic section of the MaReCo and the cylindrical section coincides at the end of the asymmetric collector.

4.1.2. Gävle

The latitude and longitude of Gävle is 60.6749 N and 17.1413 E respectively. Compared to Lisbon the location of Gävle is more north, closer to the poles where the amount of sun reached is much lesser.

4.1.2.1. Comparison of Power with respect to tilt angle

Similar simulations are performed at Gävle. The MaReCo is placed facing south with the receiver in the upper part of the collector. The Figure 4.8 shows the variation of the power output with change in tilt angle of the solar collector with respect to 20th March, 21st June, 22nd September and 21st December.

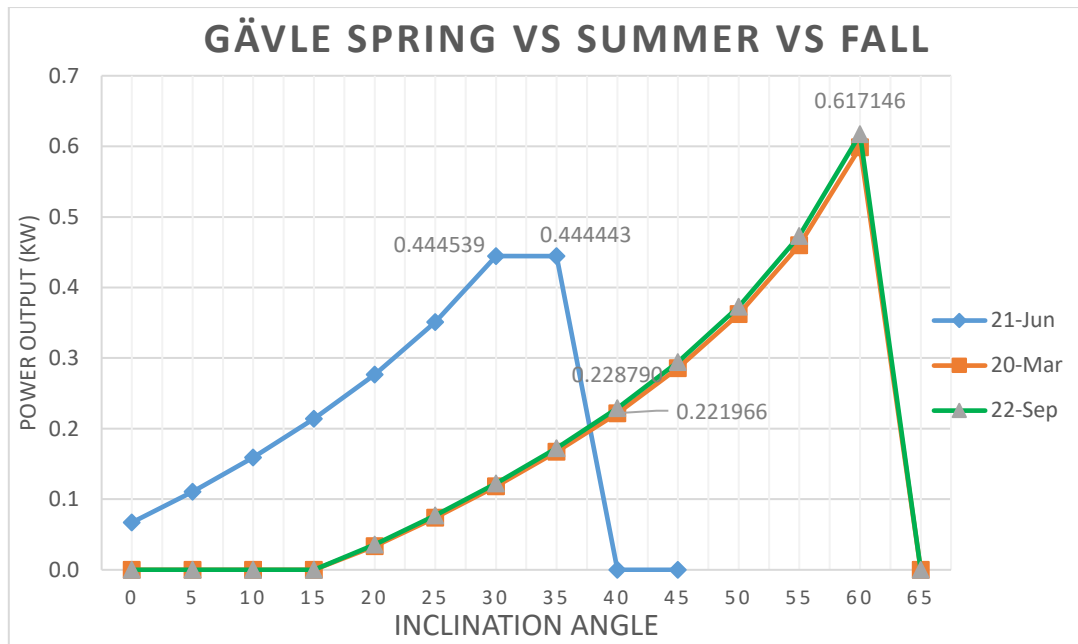


Figure 4.8 Comparison of power during 21st June, 20th March and 22nd Sept at the receiver in Gävle at 12.00 with inclination angle of the collector ranging from 0° to 65°

A similar trend shows for summer with Lisbon. The power output starts at 0°, however the break-off tilt angle is at 35°. The break-off tilt angle in Gävle in summer is higher than the cut-off tilt angle in Lisbon due to the reason that Gävle lies more north from Lisbon closer to the poles and farther away from the equator. The power output value gradually increase with the increase in the tilt angle until a break-off angle. The 20th March curve and the 22nd September curve are almost coinciding with each other. The output starts to show at 15° until the break-off tilt at 60° for both the cases. The maximum power output is seen with tilt angle 60° in 22nd September with a value of 0.61715 kW. However, due to the tilt angle of the house roofs, the power output value at 40° is 0.22879 kW in September 22nd and 0.22197 kW in March 20th. There is no curve regarding December due to no output.

4.1.2.2. Gävle summer with tilt 30° vs tilt 35°

The best possible way to tilt the solar collector in Gävle during summer is 30° [15]. However, from the Figure 4.9 the tilt angle 30° and 35° displays similar results. Simulations are performed with respect to the two angles varying the time of the day and keeping the tilt angle fixed.

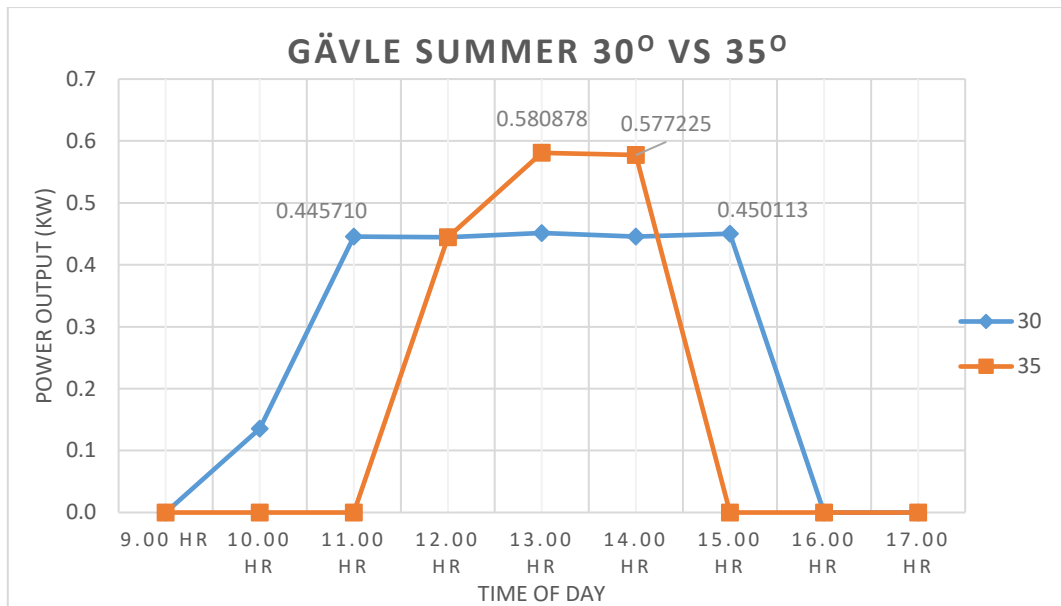


Figure 4.9 Power output (12.00 hour) vs time of day at Gävle in summer with tilt angle 30° vs tilt angle 35°

With a tilt angle of 35°, from 12:00 hour until 15:00 hour, the solar collector delivers higher power output value compared to the solar collector with tilt angle 30°. However, with a tilt angle of 30°, the collector starts to deliver output from 10:00 hour until 15:00 hour. The output power is relatively in a constant slope delivering a reliable output throughout the day.

4.1.2.3. Gävle with inverted orientation

The orientation of solar MaReCo is inverted that is facing south but the receiver is located at the lower part of the collector and placed in Gävle to check and compare the results with the previous original simulations. During winter there is no result making it unfeasible during this part of year. During spring and fall the power output starts from 65°. So the inverted orientation of the MaReCo is not suggestable. However, during summer there is a higher power output with a maximum power value of 0.52733 kW at a tilt angle of 40°.

Table 4. shows the power output (kW) at 12.00 at the receiver with tilt angle ranging from 0° to 60° during summer at Gävle with the inverted orientation.

June				
Location	Time	Day	Tilt angle	power at the receiver (kW)
Gävle	12hr	21-Jun	0	0
Gävle	12hr	21-Jun	5	0
Gävle	12hr	21-Jun	10	0
Gävle	12hr	21-Jun	15	0
Gävle	12hr	21-Jun	20	0
Gävle	12hr	21-Jun	25	0
Gävle	12hr	21-Jun	30	0
Gävle	12hr	21-Jun	35	0
Gävle	12hr	21-Jun	40	0.527333
Gävle	12hr	21-Jun	45	0.412374
Gävle	12hr	21-Jun	50	0.325859
Gävle	12hr	21-Jun	55	0.255629
Gävle	12hr	21-Jun	60	0.195650

Hence, the inverted orientation of the MaReCo is not suggestable for Gävle during spring, fall and winter. In case of summer, the inverted orientation is suitable from the collector tilt angle 40°.

4.1.3. Delhi

Delhi, the capital of India lies in the northern part of the country in the northern hemisphere. The city is situated a little north from the Tropic of Cancer. The latitude and longitude of Delhi is 28.6139 N and 77.209 E. India, a warm country by itself has a great potential for harnessing solar energy.

4.1.3.1. Comparison of power with respect to tilt angle

Simulations are performed in all the solstices, 20th March, 21st June, 22nd September and 21st December. Figure 4.10 shows the comparison of the solar power captured with respect to all the four solstices days ranging the collector tilt angle from 0° to 65°. The MaReCo is faced towards the south with the receiver at the upper part of the collector.

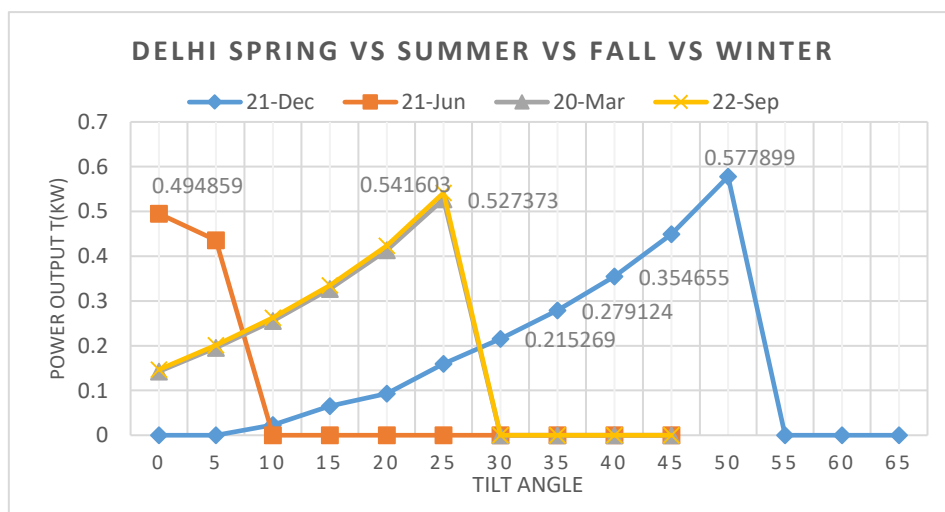


Figure 4.10 Comparison of the power during 21st June, 20th March, 22nd Sept and 21st Dec at the receiver in Delhi at 12.00 with collector tilt angle ranging from 0° to 65°

Similar to Lisbon the power output starts with a high value from 0° and break off earlier than Lisbon at 5° . This is due to the reason of the higher elevation of sun with respect to the location. The sun is much closer to the place with zenith angle of 7.3036° resulting in very high elevation. The details of the location is shown below in Figure 4.11.

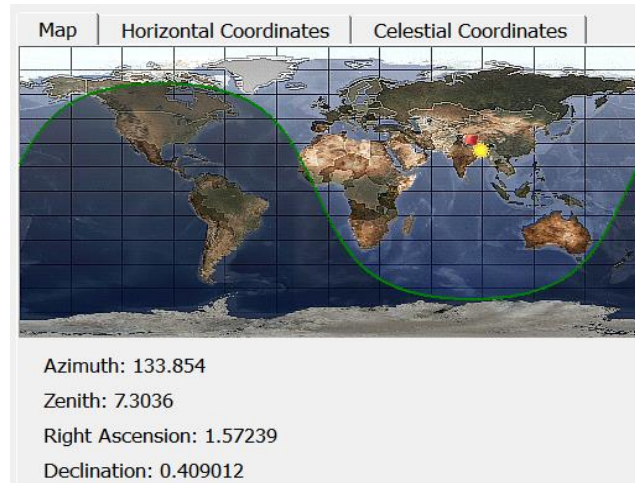


Figure 4.11 Delhi on 21st June

From the Figure 4.10, the trend in curve with respect to March and September is approximately similar. The curves almost coincide with each other. The maximum power output tilt angle of the collector during spring and fall is 25° . And during winter at a tilt angle of 40° the power output is 0.354655 kW which is a large output. Hence, the roof integrated MaReCo is suitable and applicable in Delhi with a little seasonal change in the orientation and tilt angle.

4.1.3.2. Delhi with inverted orientation in summer

The orientation of the MaReCo is inverted that is the receiver of the collector is in the lower part system. The MaReCo still faces south. Simulations are performed during summer with this orientation fixing the time of the day at 12.00 and varying the tilt angle of the collector. The resulting graph of power output vs the tilt angle is shown in Figure 4.12.

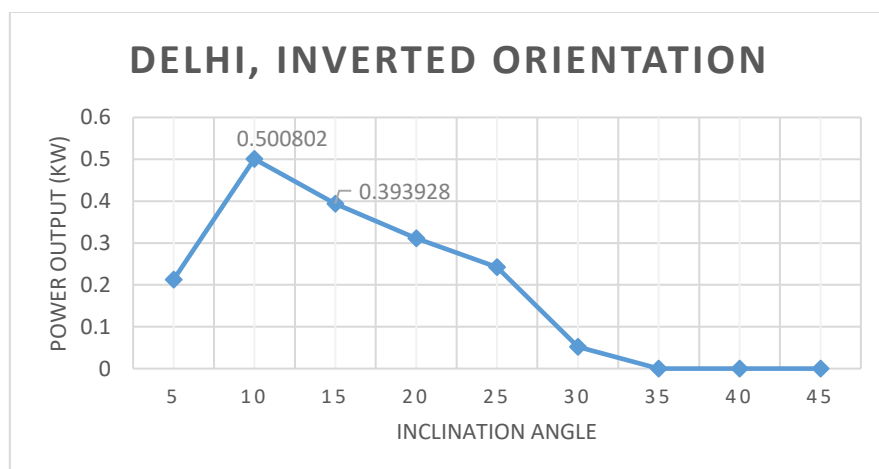


Figure 4.12. Power output (at 12.00 hour) vs inclination angle in Delhi with inverted orientation during summer of the solar MaReCo

With the orientation inverted more solar rays could enter the aperture of the solar MaReCo hence the power output is increased. At a tilt angle of 10° of the solar MaReCo, the peak output is 0.500802 kW. Therefore, the roof integrated MaReCo can be used efficiently in Delhi with an inverted orientation at an inclination angle of the collector at 10° .

4.1.3.3. Comparison of daily power curve with Lisbon in summer

The hourly curve for 21st June at an inclination of 10° vs the hourly curve in Lisbon at an inclination of 15° is shown in Figure 4.13.

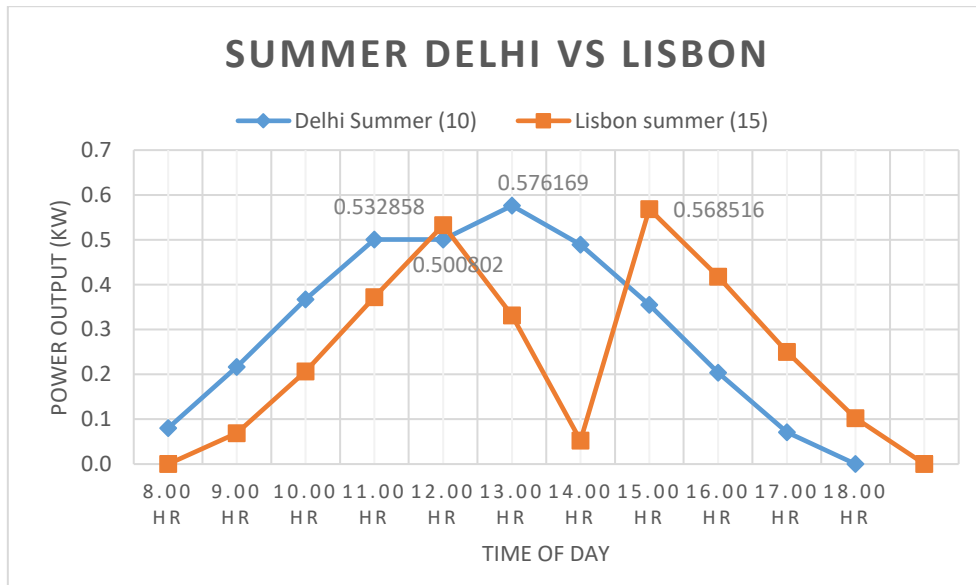


Figure 4.13 Hourly power output variation in summer in Delhi vs Lisbon

Unlike the curve trend in Lisbon, the curve trend in Delhi shows regularity. This can be explained with the position of the sun with the rising and setting of sun from east to west.

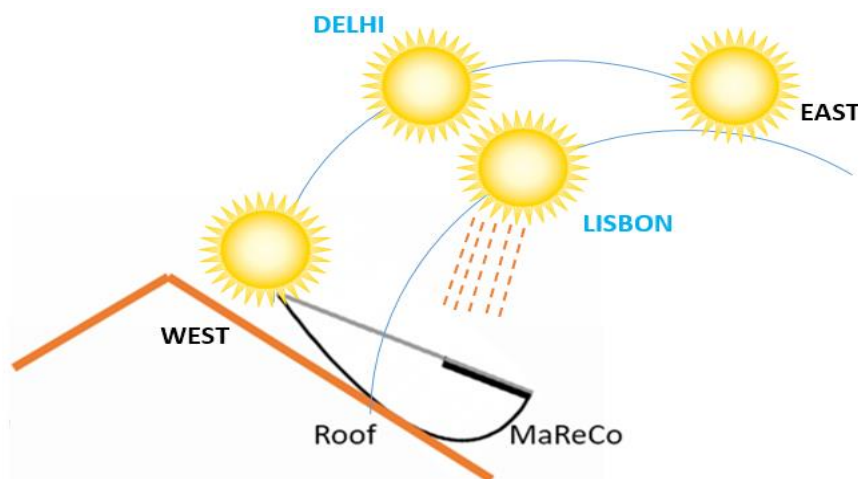


Figure 4.14 Position of the sun from rising till setting in Delhi vs Lisbon

The position of the sun during between 12.00 and 15.00 blocks the sun rays to enter the aperture of the solar collector resulting in less output. The zenith angle of Delhi on 21st June is 7.3036° from Figure

4.11 and zenith angle of Lisbon on the same day is 25.885°. Hence, the sun is higher in Delhi. So regardless of the time of the day the solar rays enters freely into the aperture of the collector resulting in a regular power curve as shown in Figure 4.14.

4.1.3.4. Delhi with inverted orientation in spring, fall and winter

Simulations are done with the collector being inverted during spring, fall and winter. During winter the output power is not significant hence, it is not recommended. However, during spring and fall at a tilt angle of 30°, the power output starts with a maximum value of 0.60144 kW and 0.59887 kW respectively. The value gradually decreases as the tilt angle is increased. Therefore, for Delhi, the standard MaReCo gives promising power output with the inverted orientation during spring, summer and fall. For winter the normal orientation shows reliable power output. Hence, MaReCo is suitable in Delhi with lesser latitude than Lisbon.

4.2. Modified roof integrated MaReCo

The redesigned MaReCo structure has the receiver position in such a way that the middle part of the receiver is aligned at the intersection plane of the cylindrical part and the parabolic trough. The idea is to try to increase the amount of photons received on the absorber as much as possible with the receiver at the focus.

4.2.1. Comparison of power with respect to the tilt angle

Similar simulations are made with the time of the day fixed at 12.00 and varying the angle of inclination of the collector for the four solstices, 21st June, 20th March, 22nd September and 21st December. The collector is faced south and the receiver is in the upper part of the collector. The resulting curve is shown in Figure 4.15.

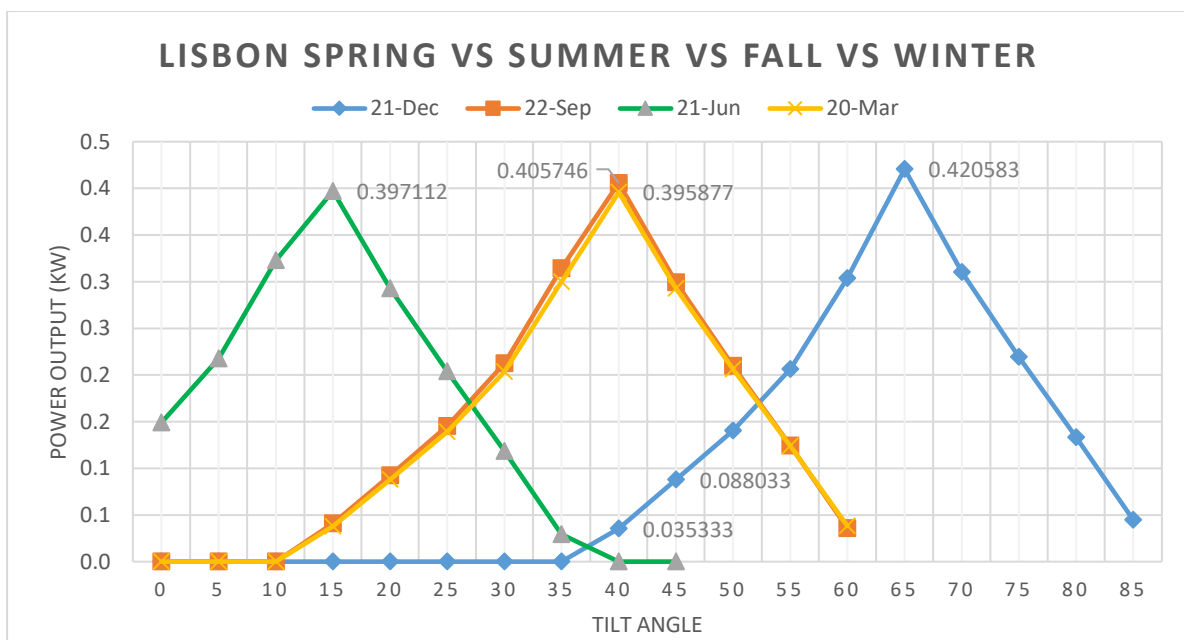


Figure 4.15 Comparison of the power during 21st June, 20th March, 22nd Sept and 21st Dec at the receiver in Lisbon at 12.00 with inclination of angle of the collector ranging from 0° to 85°

The curve shows a similar fashion. There is no peculiar curve trend. All the maximum output are the same. The summer curve as usual starts from a lower inclination and then the spring and fall curve leading to finally the winter curve starting from 40°. The maximum power output is 0.397112 kW at 15° in summer in Lisbon which is lesser than the actual roof integrated MaReCo design (from section 4.1.1). The average roof angle is in between 10° to 40°. Hence, this designed can be effectively used in spring, fall and summer but not so efficiently during winter.

4.2.2. Hourly simulation in summer

Figure 4.16 shows the curve during summer at 15° angle of inclination.

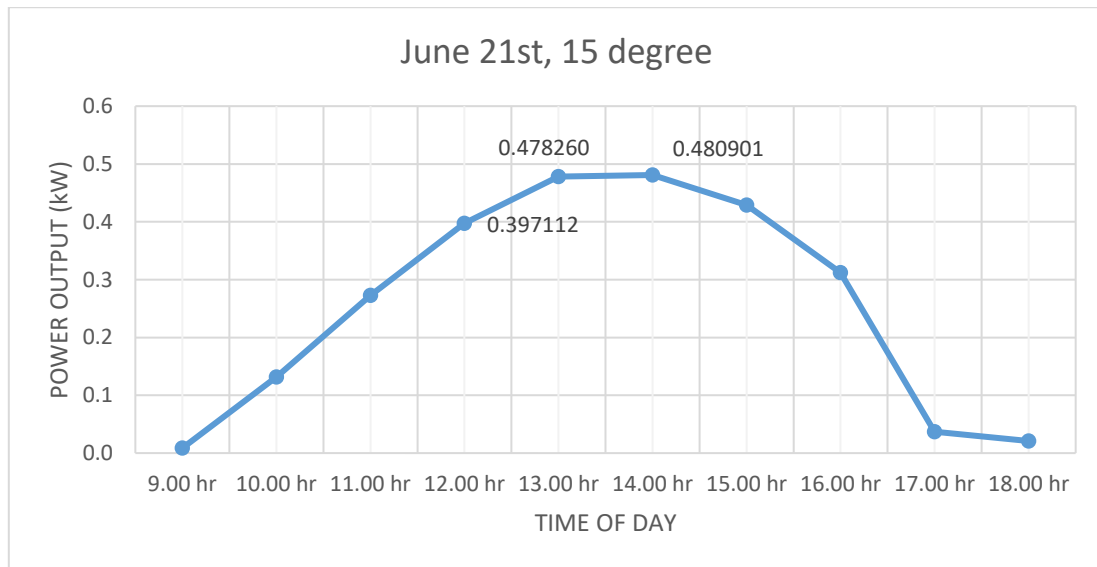


Figure 4.16 Hourly power output (kW) in 21st June in Lisbon at 15° collector inclination

The curve trend is smooth and gives a reliable output throughout the day. It reaches its maximum output at 14.00 unlike the normal roof integrated MaReCo in Lisbon during summer.

4.2.3. Flux distribution on the receiver

Figure 4.17 shows the flux distribution of the solar rays on the receiver of the modified MaReCo.

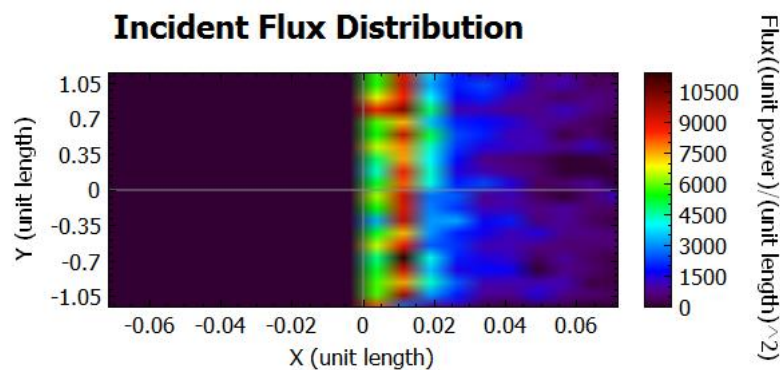


Figure 4.17 Flux distribution on 21st June in Lisbon

The solar rays are concentrated on the middle part of the receiver spreading from the right side. The left side of the receiver lacks the concentration of reflected solar rays from the collector.

4.2.4. Inverted orientation of modified roof integrated MaReCo

4.2.4.1. Power vs inclination

The collector is inversely oriented that is the receiver part of the system stays on the both still facing the south. Figure 4.18 shows the simulations done in Lisbon with the modified MaReCo during summer, spring and fall.

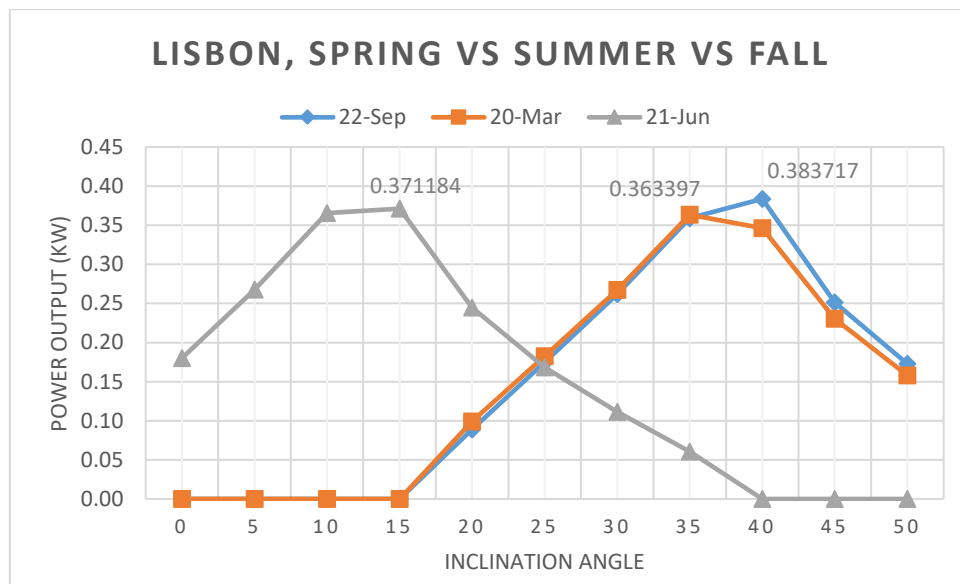


Figure 4.18 Comparison of the power during 21st June, 20th March and 22nd Sept at the receiver in Lisbon at 12.00 with inclination of angle of the collector ranging from 0° to 50°

The inverted orientation of the modified MaReCo shows worse result than the normal orientation. The maximum output power for each season decreases. Regarding winter the power output starts from 45° and reaches a maximum value at an inclination of 65°. Therefore, this orientation is not recommended.

4.3. Parabolic Collector with side edge receiver

The position of the sun in the equatorial region barely changes. Keeping the area of the aperture of the collector the same, symmetrical parabolic collectors are designed for such regions. Symmetrical parabolic collectors are less complicated and easier to manufacture. On top of that the solar energy is easily available in equatorial regions and therefore provides a bigger market potential.

Here the receiver is located at the side edge of the collector. The feasibility of the parabolic collector with the side edge receiver is checked in Lisbon and Nairobi a city close to the equator.

4.3.1. Lisbon

4.3.1.1. Simulations with normal and inverted orientation in summer

Two sets of simulations are performed during the summer in 21st June with the two orientations, normal and inverted, of the collector (as discussed in section 4.1.1.1). Figure 4.19a is with respect to the normal orientation and Figure 4.19b with the inverted orientation.

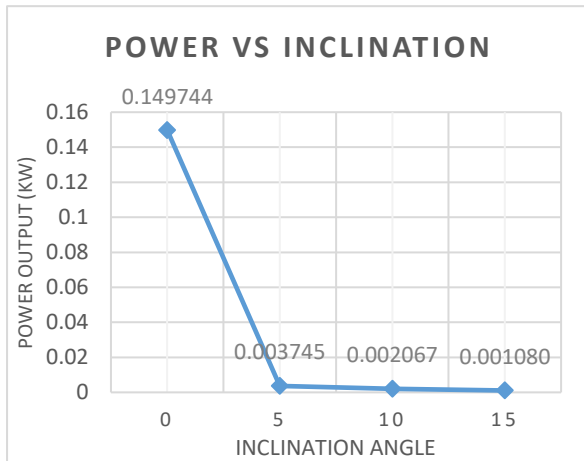


Figure 4.19a. Power vs inclination with normal orientation

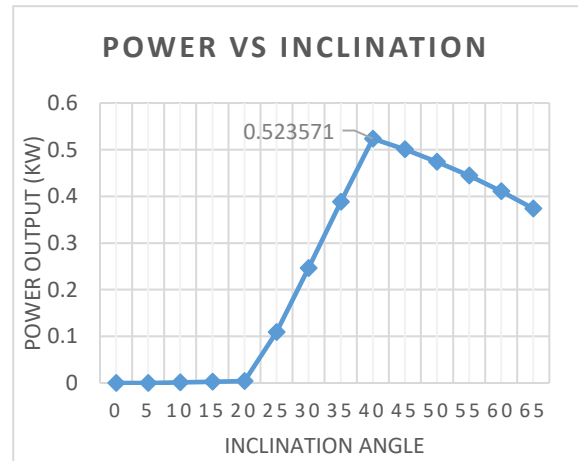


Figure 4.19b. Lisbon, inverted orientation

As usual the power vs inclination curve with the normal orientation breaks off early, here after 0°. An efficient and useful power output can be obtained when the parabolic solar collector with receiver at the side edge is oriented inverted from the normal way. The maximum power output, 0.523571 kW, is obtained at 40° during summer in Lisbon. Comparing with the roof integrated MaReCo, the maximum power output with a value of 0.532858 kW is received at a tilt angle of 15° with the inverted orientation. The feasibility and effective usability of the two designs is that the tile angle of the collector has to be 40 or greater.

4.3.1.2. Comparison of power with respect to inclination angle

The Figure 4.20 shows the power curve with respect to the inclination angle during spring, fall and winter. The collector is faced normally towards south with the receiver at the upper part of the collector

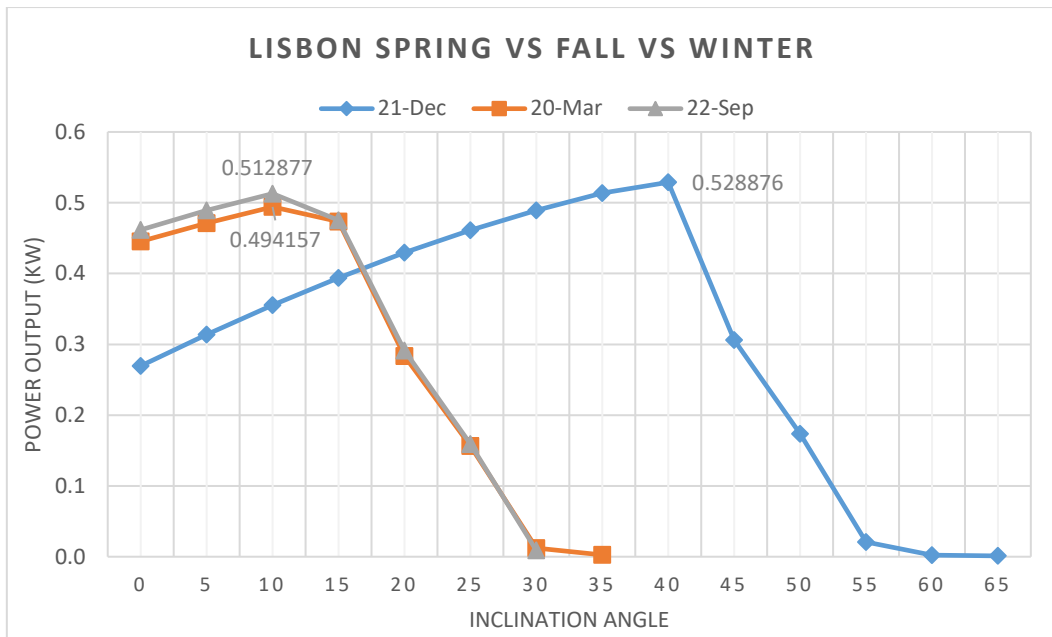


Figure 4.20 Comparison of the power during 20th March, 22nd Sept and 21st Dec at the receiver in Lisbon at 12.00 with inclination angle of the collector ranging from 0° to 65°

The power output starts at a lower tilt angle of the receiver for all the curves reaching maximum output at 10° for spring and fall and 40° for winter. The curve depicting spring and fall are almost identical as usual. The design is very well suited for spring and fall. However, for summer and winter unless the house roof angle is less than 40°, the parabolic collector with side edge receiver is well suitable.

4.3.1.3. Flux distribution on the receiver

The flux distribution of the solar radiation on the receiver during summer at the tilt angle of 40° is shown in Figure 4.21.

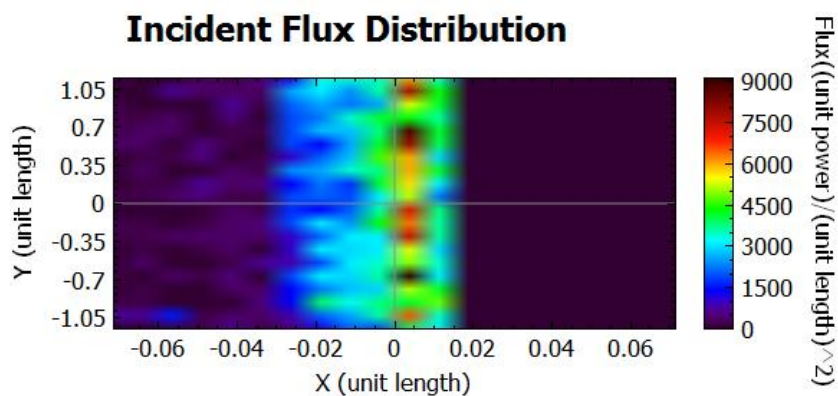


Figure 4.21 Flux distribution during summer on side edge receiver of parabolic collector in Lisbon

Most of the rays fall on the middle part of the receiver extending from the right end. Negligible rays are reached at the left end of the receiver.

4.3.2. Nairobi

Nairobi, the capital city of Kenya in Africa lies very close to the equator with latitude and longitude 1.2921° S and 36.8219° E respectively.

4.3.2.1. Comparison of power with respect to inclination angle

The Figure 4.22 shows the comparison of the four seasons in Nairobi at 12.00 with varying angle of inclination of the collectors. Regarding Nairobi, since it is located at the equatorial region the orientation of the collector is of less factor to consider. Hence, the solar collector is oriented in the best output condition.

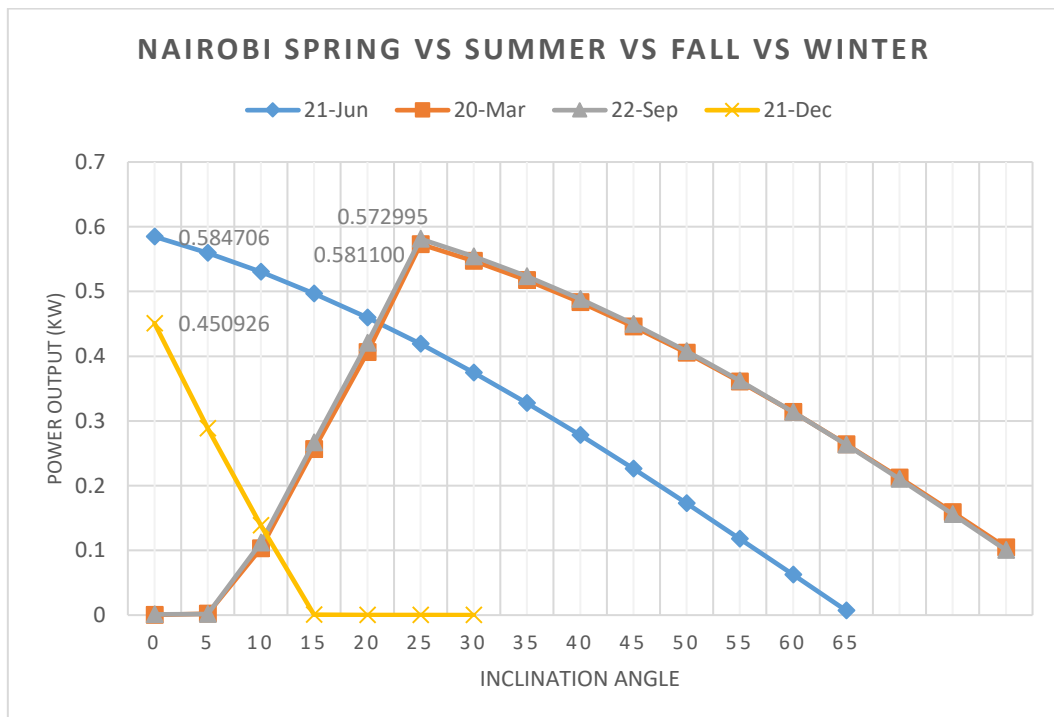


Figure 4.22 Comparison of the power during 21st June, 20th March, 22nd Sept and 21st Dec at the receiver in Nairobi at 12.00 with inclination angle of the collector ranging from 0° to 65°

The power outputs starts very early for all the four seasons in Nairobi. This is because of the high elevation position of the sun near the equator. The maximum output at summer is obtained at 0° inclination with a value of 0.584706 kW. The curve trend of spring and fall shows identical behaviour with maximum power output angle at 25°. Moreover, the angle of inclination for maximum power output for December is 0°. Hence, the parabolic collector with side edge receiver is very feasible for locations near the lower latitude for all the seasons.

4.3.2.2. Flux distribution on the receiver

The flux distribution of the solar rays on the side edge receiver of the parabolic receiver is shown in Figure 4.23.

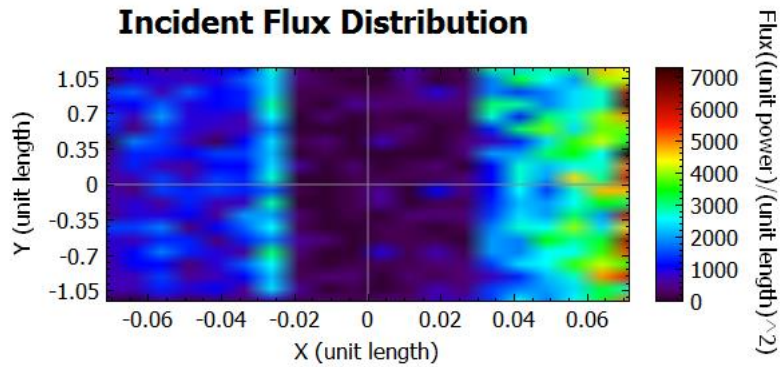


Figure 4.23 Flux distribution during summer on side edge receiver of parabolic collector in Nairobi

For a symmetrical parabolic collector the solar flux distribution is seen throughout the receiver. Most of the rays fall on the right end of the receiver.

4.4. Parabolic collector with horizontal receiver at the focus

The collector has a symmetrical parabolic structure with the receiver at the horizontal focus of the collector. Simulations are performed at Lisbon and Nairobi to check the feasibility and usability of the collector.

4.4.1. Lisbon

4.4.1.1. Comparison of power with respect to inclination angle

Similar simulations are executed with the parabolic collector with horizontal receiver at the focus at Lisbon, fixing the time of the day at 12.00 and varying the angle of inclination of the collector from 0° to 90°.

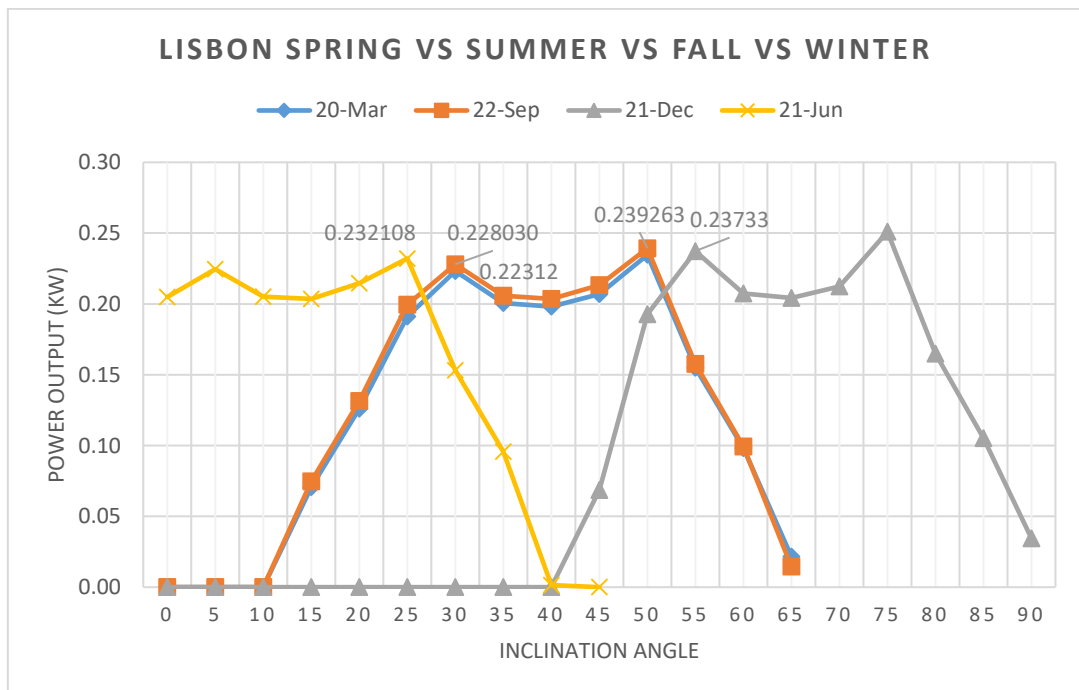


Figure 4.24 Comparison of the power during 21st June, 20th March, 22nd Sept and 21st Dec at the receiver in Lisbon at 12.00 with inclination angle of the collector ranging from 0° to 90°

The curves shows identical behaviour in all the four solstices. There is a decrease in the power output after a peak output in each case leading to another peak power output. This is due the reason that the collector when inclined in a manner collects more solar rays enter the aperture in one side, since the receiver is situated in the middle. The solar rays are then blocked by the receiver to enter the aperture when the collector is inclined more with respect to the ground until the next point of inclination where majority of the solar rays can enter the other opening.

Compared to the previous collectors, the power output is lesser. However, the inclination angle where the peak power output exist during summer, spring and fall is almost the same which is a huge advantage compared to previous collectors, since the user need not bother with the tilt of the collector. The collector is not usable during winter as it starts to produce output after 40° which would be the main drawback of this design. On the other hand the collector produces a higher output during winter at an angle almost near the right angle which makes the collector similar as a wall MaReCo.

4.4.1.2. Flux distribution on the receiver

Figure 4.31 shows the flux distribution of the solar rays at the horizontal receiver of parabolic collector during summer in Lisbon at a collector tilt angle of 25°.

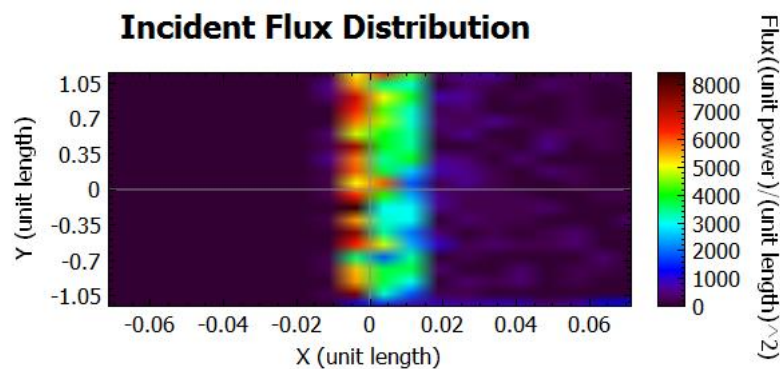


Figure 4.25 Flux distribution on 21st June in Lisbon

Most of the rays are focused at the middle part of the receiver. The left part of the receiver lacks solar rays compared to the remaining part.

4.4.2. Nairobi

4.4.2.1. Comparison of power with respect to inclination angle

To check the suitability in the equatorial region of the parabolic symmetrical collector with the horizontal receiver at the focus, simulations are performed at Nairobi fixing the time of the day at 12.00 and varying the tilt angle of the collector.

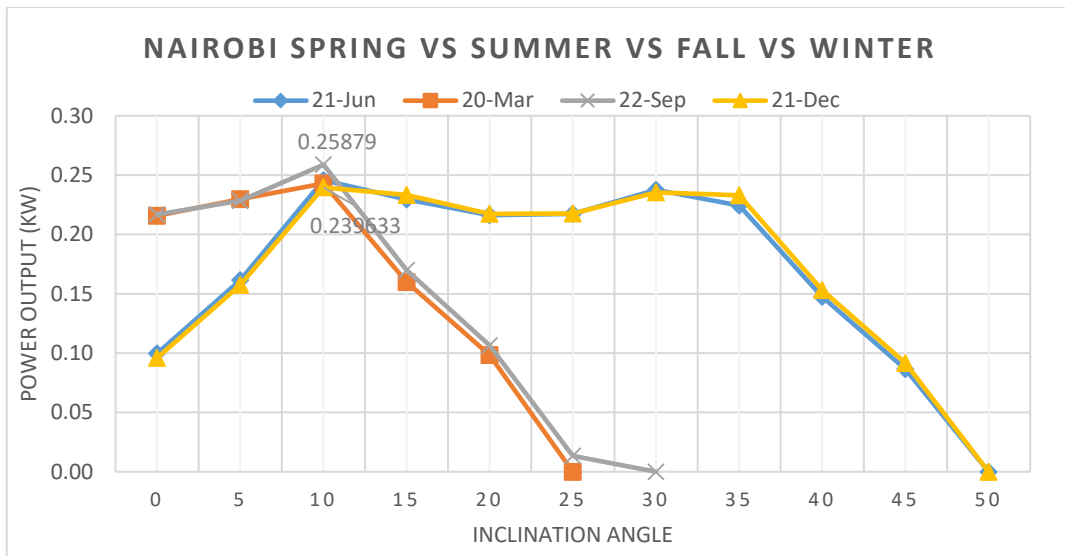


Figure 4.26 Comparison of the power during 21st June, 20th March, 22nd Sept and 21st Dec at the receiver in Nairobi at 12.00 with inclination angle of the collector ranging from 0° to 50°

The peak power output is quite less with a maximum value of 0.25879 kW at June 21st. The curve trend of summer and winter are almost the same in this situation. The same goes with the curve trend of September and March. The tilt angle of the collector at which the peak power can be achieved is 10° for all the four solstices, which is being the best factor of this collector. It ensures that the collector can stay as it is for the whole year with very little change saving time for extra maintenance.

4.4.2.2. Comparison of parabolic collector with horizontal middle receiver with modified MaReCo

The power vs inclination curve for the modified MaReCo at Nairobi is given in Figure 4.33. The collector is fixed with inverted orientation throughout the season.

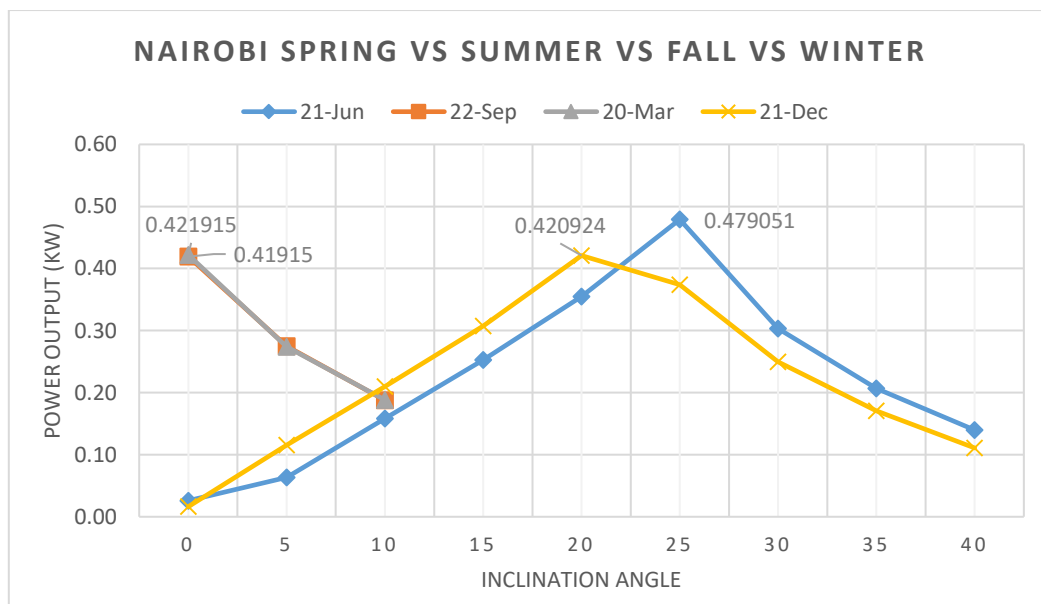


Figure 4.27 Comparison of the power during 21st June, 20th March, 22nd Sept and 21st Dec at the receiver in Nairobi at 12.00 with inclination angle of the collector ranging from 0° to 40°

The curve trend for summer and winter is identical with the maximum power output at an inclination angle of 25° and 20° respectively. For spring and fall the curve is also almost coinciding with the maximum output at an inclination angle of 0°. The output power of the modified MaReCo compared to parabolic collector with horizontal middle receiver is much larger. Apart from the fact that the modified MaReCo requires change in inclination angle throughout the seasons, it is suitable for all the seasons. Hence, modified MaReCo is more preferable than the parabolic collector with middle horizontal receiver.

4.4.2.3. Flux distribution on the horizontal middle receiver of the parabolic collector

Figure 4.34 shows the flux distribution of solar rays on the middle horizontal receiver of the parabolic collector during summer at 10° tilt angle.

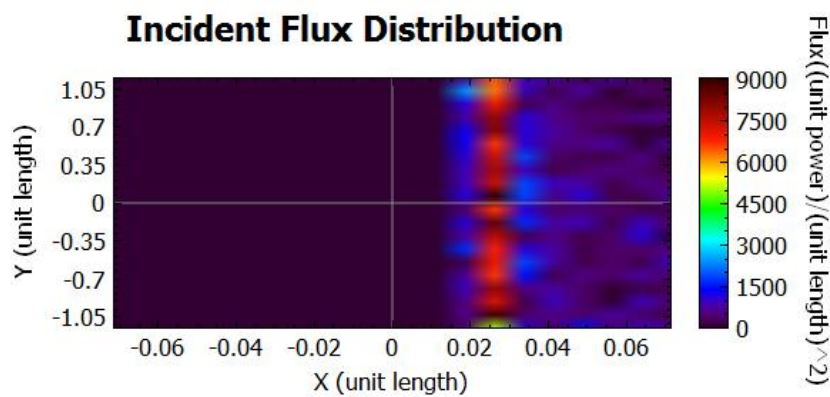



Figure 4.28 Flux distribution on 21st June in Nairobi

The flux strength is less and is spread on the right part of the receiver.

4.6. Comparison

Table 6. Comparison between the designs

Simulation structure		Max. power output inclination angle			Feasibility and suitability
 Roof Integrated MaReCo	Month	Lisbon	Delhi	Gävle	Lisbon: Better results in spring, fall and summer with inverted orientation Gävle: Better results in summer with inverted orientation, not suitable for winter Delhi: Perfect for all seasons, better with inverted orientation during summer, spring and fall
	Mar 20	35	25	60	
	June 21	15	10	30	
	Sept 22	35	25	60	
	Dec 21	60	50	n/a	





 <p>Redesigned MaReCo</p>	Month	Lisbon	Nairobi	<p>Lisbon: Suitable for spring, summer and fall but lesser output than actual roof integrated MaReCo, not suitable for winter</p> <p>Nairobi: Suitable for all the seasons</p>
	Mar 20	40	0	
	June 21	15	25	
	Sept 22	40	0	
	Dec 21	65	25	
 <p>Parabolic Collector with side edge receiver</p>	Month	Lisbon	Nairobi	<p>Lisbon: Suitable for all the seasons, better output than standard MaReCo, works best for winter</p> <p>Nairobi: Perfect for all the seasons</p>
	Mar 20	10	25	
	June 21	40	0	
	Sept 22	10	25	
	Dec 21	40	0	
 <p>Parabolic Collector with horizontal receiver</p>	Month	Lisbon	Nairobi	<p>Lisbon: Lesser output compared to other models, greatest advantage is that it does not need to change the collector tilt angle for spring, summer and fall, in winter it acts like a wall MaReCo</p> <p>Nairobi: Lesser output compared to other models, no need to change the tilt angle throughout the year, Modified MaReCo in Nairobi gives better output</p>
	Mar 20	30, 50	10	
	June 21	25	10,30	
	Sept 22	30, 50	10	
	Dec 21	55, 75	10,30	

Table 7. Comparison between normal and inverted orientation of roof integrated MaReCo

	Gävle	Tilt angle		Power (kW)
	Normal orientation	Mar 20 th	60	0.59844
		June 21 st	30	0.44454
		Sept 22 nd	60	0.61715

 Roof Integrated MaReCo		Dec 21 st	n/a	n/a
	Inverted orientation	Mar 20 th	n/a	n/a
		June 21 st	40	0.52733
		Sept 22 nd	n/a	n/a
		Dec 21 st	n/a	n/a
	Lisbon	Tilt angle		Power (kW)
	Normal orientation	Mar 20 th	35	0.46189
		June 21 st	10	0.48995
		Sept 22 nd	35	0.40256
		Dec 21 st	60	0.47332
	Inverted orientation	Mar 20 th	40	0.52881
		June 21 st	15	0.53286
		Sept 22 nd	40	0.54344
		Dec 21 st	n/a	n/a
	Delhi	Tilt angle		Power (kW)
	Normal orientation	Mar 20 th	25	0.52737
		June 21 st	5	0.43547
		Sept 22 nd	25	0.54160
		Dec 21 st	50	0.57790
	Inverted orientation	Mar 20 th	30	0.60143
		June 21 st	10	0.50080
		Sept 22 nd	30	0.59887
		Dec 21 st	n/a	n/a

4.7. Proposal

The multiple changes in parameters, location, tilt angle, orientation of the collector, time of day, season, in the thesis work make it difficult to conclude with the best situation. However, individual conclusions with specific scenarios can be achieved.

For Gävle, the normal orientation works best for spring and fall and inverted orientation for summer but after an inclination of 40°. However, for lower latitude places like Lisbon and New Delhi, the inverted orientation gives better output power than the normal orientation for summer, spring and fall. The performance of a standard MaReCo is increased with a slight change in the orientation. Inverting the orientation of the collector that is the collector still faces south (in the northern hemisphere) but the receiver is at the lower part of the system, the output can be increased further. As the location proceeds towards the equatorial region, from Gävle, Lisbon and Delhi, the performance of the MaReCo increase. Hence, inverted orientation is proposed for lower latitude regions with a MaReCo design.

The modified MaReCo is not a recommended design over the conventional MaReCo but can be used in equatorial region. It performs better than a parabolic collector with middle horizontal receiver.

The parabolic collector with side edge receiver is most recommended model for equatorial regions, better than parabolic collector with horizontal receiver. It is suitable for all the seasons. The design also gives better result in Lisbon than the standard MaReCo. Therefore, for lower latitude regions the proposed collector structure is the parabolic collector with side edge receiver.

Parabolic collector with horizontal middle receiver is not a recommendation for any location on the globe, although it provides its performance without the need to change its orientation or tilt angle throughout the year.

5. Future work:

Much of the thesis work done is regarding the simulations with respect to possible solar collector models in various locations in the world. Many factors are yet to consider and many promising ways to improve the efficiency and power output of the collector still exists. The following points describes the possible improvements and future works which can be perform to make a solar collector efficient with low cost and maintenance –

- The influence of the optical properties of the receiver and the collector constituents can be considered to make the model as realistic as possible. The simulations performed in the thesis work is an ideal case with the reflectivity of the collector taken as 1.
- Simulations can be made with different materials at different times of the day and conditions of year considering the price factor of the materials. The dependence of the type of material with the power output can be studied in the future.
- The strings of cell of the receiver is non-uniform. This factor is not taken into consideration in the thesis work. Future work can include this condition and also analyse an in-depth 3-D details of the receiver during the working hours of the collector.
- The positions of the receiver in the collector can be varied more and studied further with respect to different time, day and places of the world.
- The thermal heat involved in the solar collector is not considered. A huge factor to be considered in the future to improve the efficiency and feasibility of a solar PVT collector.
- The simulations in the thesis work are performed in ideal conditions of the day and weather with an ideal case of maintenance. More realistic simulations can be made taking changes in weather and maintenance of the collector during those conditions in consideration.

6. Conclusion

The thesis work is mostly simulation based done with unique solar collector models. The work give rise to some significant results and modifications which can be made to improve the output. The simulations are performed in various locations in the world to ensure the feasibility and suitability of the solar collector model in different parts of the globe. The next step to simulations is experimental proof to compare the real time values with the simulated results. However the importance of simulation lies much deeper than perceived. It is a very powerful tool to expose the design model to divergent conditions with no caution of accidents to consider whatsoever ensuring a very safe conditions at almost free of cost. Simulation can be perceived as an investment which will be fruitful in the future and save the user from various problems and difficulties.

The PowerCollector MaReCo from Solarus is a roof integrated model. The market already exist in various places in Europe, Africa and also India. Various simulations are performed with this design in Gävle, Lisbon and Delhi. The actual real time result from the company regarding Gävle goes very well with the simulation results. In case of Lisbon and Delhi where the elevation of the sun is higher than Gävle, the thesis work includes result where a little shift in orientation of the solar collector can result huge improvement with no extra cost. The solar MaReCo still faces south but in the inverted position as described in section 4.1.1.2. A higher output is obtained with the same solar collector. This result can be implemented directly to experimental testing in real site to check the definiteness of the simulations.

Four more solar collectors are modelled and simulated in different conditions of the year at different locations. A slight change in the position of the receiver of the roof integrated MaReCo is remodelled. The shift in the location of the receiver made the collector give lower output power. On top of that, it is not suitable for winter. Hence, the modified MaReCo model is not recommended.

The position of the sun barely changes in the equatorial region. Moreover, the market potential is huge due to long hours of warm sun year round. Keeping the area of aperture of the collector in check, symmetrical parabolic collectors are designed for such regions. The cost of production is proposed to be approximately similar since additional materials are not used. Simulations are performed at Nairobi, the capital of Kenya which is located at the equatorial region.

The parabolic collector with receiver at the side edge is the best suitable solar collector not only for equatorial region but also for places with lower latitude. The roof integrated MaReCo has difficulties producing effective results during winter. However, the parabolic collector with side edge receiver is feasible with better output than MaReCo during winter.

Lastly but not the least, the parabolic collector with horizontal receiver in the focus gives lesser output than all the other mentioned collectors. The advantage of the receiver is that the user can focus the solar collector about a definite tilt angle throughout the year reducing the maintenance.

Although there exist a lot of rooms to improve the output and the effectiveness of the solar models, the simulation results obtained in the thesis work can serve as an important proposition for the following

step to be taken. It can be used as a guide post for the next set of simulations and future works proposed which would take part in shaping the future energy demand leading towards a reliable and carbon free environment.

Bibliography:

[1] 2016, *Snapshot of global photovoltaic markets*

[http://www.iea-pvps.org/fileadmin/dam/public/report/statistics/IEA-PVPS -
_A Snapshot of Global PV - 1992-2016_1_.pdf](http://www.iea-pvps.org/fileadmin/dam/public/report/statistics/IEA-PVPS_-_A_Snapshot_of_Global_PV_-_1992-2016_1_.pdf)

[2] Eurostat, statistics explained: *File:Share of electricity from renewable sources in gross electricity consumption, 2004-2015 % T2 New.png* [26/12/2017]

[http://ec.europa.eu/eurostat/statistics-
explained/index.php/File:Share of electricity from renewable sources in gross electricity consum
ption,2004-2015_%25_T2_New.png](http://ec.europa.eu/eurostat/statistics-explained/index.php/File:Share_of_electricity_from_renewable_sources_in_gross_electricity_consumption,2004-2015_%25_T2_New.png)

[3] Zweibel, K., 2005. "The Terawatt challenge for thin film PV". In: Poortmans, J., Archipov, V. (Eds.), *Thin Film Solar Cells: Fabrication, Characterization and Application*. John Wiley, pp. 18–22

[4] Kazmerski, L., 2006. "Solar photovoltaics R&D: at the tipping point: a 2005 technology overview". *Journal of Electron Spectroscopy and related Phenomena* 150 (2–3), 105–135.

[5] *Concentrating Solar Power (CSP) Technologies*, [26/12/2017]

<http://solareis.anl.gov/guide/solar/csp/>

[6] Herrando M., Markides C., 2016. "Hybrid PV and solar-thermal systems for domestic heat and power provision in the UK: Techno-economic considerations". *Journal of Applied Energy* 161, 512–532.

[7] Duffie, J. A., Beckman, W.A., 2013. "Solar Engineering of Thermal Processes", 4th edition. John Wiley & Sons

[8] *Solar Energy* [22/12/2017]

<http://www.inforse.org/europe/dieret/Solar/solar.html>

[9] *Solar Radiation Basics* [22/12/2017]

<http://solardat.uoregon.edu/SolarRadiationBasics.html>

[10] *Solarus* [22/12/2017]

<http://solarus.com/>

[11] *The new power to fuel our future*. [13/12/2017]

<http://solarus.com/wp-content/uploads/2017/05/Solarus-Brochure-Web-2017.pdf>

[12] *Solarus AB* [10/12/2017]

<http://www.nordicgreen.net/startups/solar/solarus-ab>

[13] *Flat Plate Solar Collectors* [25/12/2017]

http://www.flasolar.com/active_dhw_flat_plate.htm

[14] *Flat Plate Solar Collector* [13-12-2017]

<https://solartribune.com/solar-flat-plate-collector/>

[15] Adsren, M. 2002. "Solar thermal collectors at high altitudes-Design and performance of non-tracking concentrators". Acta Universitatis Upsaliensis. *Comprehensive Summaries of Uppasala Dissertations from the Faculty of Science and Technologies* 697. 78pp. Uppasala. ISBN 91-554-5274-4

[16] *Climate Kids, NASA* [13-12-2017]

<https://climatekids.nasa.gov/concentrating-solar/>

[17] Günther, M. Shahbazfar, R., "Advanced CSP Teaching Materials", chapter 7: Solar dish technology

<http://www.energy-science.org/bibliotheque/cours/1361450770Chapter%2007%20dish.pdf>

[18] *Solarpaces/Estela/Greenpeace (2009): Concentrating Solar Power. Global Outlook 09*

<http://www.greenpeace.org/international/Global/international/planet-2/report/2009/5/concentrating-solar-power-2009.pdf>

[19] Häberly, A., 2012. "Linear Fresnel Collectors. Encyclopaedia of Sustainability Science and Technology", Springer New York, 6031–6037.

[20] Puerto, J. M. "Performance Evaluation of the Solarus AB Asymmetric Concentrating Hybrid PVT Collector", Ph.D. Thesis, 2013-2014.

<http://www.diva-portal.org/smash/get/diva2:727716/FULLTEXT01.pdf>

[21] *Concentrating collectors* [5/10/2017]

<http://www.powerfromthesun.net/Book/chapter09/chapter09.html>

[22] *The new power to fuel our future (technical brochure)*

<http://solarus.com/wp-content/uploads/2017/08/Solarus-Technische-Brochure-web-v1.pdf>

[23] Blanco, M.J. *Tonatiuh: "An object oriented, distributed computing, Monte-Carlo ray tracer for the design and simulation of solar concentrating systems"*, The University of Texas at Brownsville, Brownsville, Texas

[24] *Iat-Cener/Tonatiuh, Home* [9/12/2017]

<https://github.com/iat-cener/tonatiuh/wiki>

[25] *Tonatiuh*

http://secure.cener.com/documentos/F_Tonatiuh.pdf

[26] *Iat-Cener/Tonatiuh, Output files format* [10/12/2017]

<https://github.com/iat-cener/tonatiuh/wiki/Output-files-format>

[27] *Wolfram Mathematica* [10/12/2017]

<https://www.wolfram.com/mathematica/>

[28] *Iat-Cener/Tonatiuh, Tutorial ParabolicDish V201* [11/12/2017]

<https://github.com/iat-cener/tonatiuh/wiki/Tutorial-ParabolicDish-V201>

[29] *Greenenergy star* [11/12/2017]

<http://www.greenergystar.com/shop/content/14-optimizing-pv-array>

[30] Jia, Y., "*Quaternion and Rotation*", Com S 477/577 Notes, [05/09/2017]

<http://web.cs.iastate.edu/~cs577/handouts/quaternion.pdf>